FEDERAL UNIVERSITY OF SANTA CATARINA
JOINVILLE TECHNOLOGY CENTER
POS-GRADUATION PROGRAM OF ENGINEERING AND MECHANICAL SCIENCES

Paulo Rafael Alberton Bloemer

Rapid Methodology for Vehicle Dynamic Parameter Estimation

Joinville
2024

Paulo Rafael Alberton Bloemer

Rapid Methodology for Vehicle Dynamic Parameter Estimation

Master Thesis of Pos-Graduation Program of Engineering and Mechanical Sciences of Joinville Technology Center of Federal University of Santa Catarina to obtain the title of Master Mechanical Engineering and Sciences.
Supervisor:: Prof. Thiago Antônio Fiorentin, Dr.

Joinville
2024

Ficha catalográfica gerada por meio de sistema automatizado gerenciado pela BU/UFSC.
Dados inseridos pelo próprio autor.

Bloemer, Paulo Rafael Alberton
Rapid Methodology for Vehicle Dynamic Parameter Estimation / Paulo Rafael Alberton Bloemer ; orientador, Thiago Antônio Fiorentin, 2024.
86 p.

Dissertação (mestrado) - Universidade Federal de Santa Catarina, Campus Joinville, Programa de Pós-Graduação em Engenharia e Ciências Mecânicas, Joinville, 2024.

Inclui referências.

1. Engenharia e Ciências Mecânicas. 2. Dinâmica veicular. 3. Estimativa de parâmetros. I. Fiorentin, Thiago Antônio. II. Universidade Federal de Santa Catarina. Programa de Pós Graduação em Engenharia e Ciências Mecânicas. III. Título.

Paulo Rafael Alberton Bloemer

Rapid Methodology for Vehicle Dynamic Parameter Estimation

This Master Thesis was considered suitable for obtaining the title of "Master Mechanical Engineering and Sciences" and approved in its final form by Pos-Graduation Program of Engineering and Mechanical Sciences.

Joinville, Jul 12th, 2024.

Documento assinado digitalmente
Roberto Simoni
Data: 12/09/2024 11:04:28-0300
CPF: ***.398.969-**
Verifique as assinaturas em https://v.ufsc.br

Prof.Roberto Simoni, Dr.
Coordenador of the course

Examination Board:

Documento assinado digitalmente
Thiago Antonio Fiorentin
Data: 11/09/2024 10:46:50-0300
CPF: ***.053.219-**
Verifique as assinaturas em https://v.ufsc.br

Prof. Thiago Antônio Fiorentin, Dr.
Supervisor:

Prof. Andrea Carboni Piga, Dr.
Appraiser
Federal University of Santa Catarina

Prof. Marcos Alves Rabelo, Dr.
Appraiser
Federal university of Santa Catarina

Prof. Fernando Humel Lafratta , Dr.
Appraiser
Santa Catarina University State

ACKNOWLEDGEMENTS

I am grateful for the unwavering support of my parents, Mateus Bloemer and Luzia Biancato Alberton, and my girlfriend, Bianca Michels Albino, throughout this endeavor.

Special appreciation goes to my advisor, Dr. Thiago Antonio Fiorentin, for his guidance, availability, and enthusiasm, which continually motivated me even during challenging times.

I extend my gratitude to my colleagues Maikol Drechsler, Yuri Poledna, and Leticia Cristofolli for their assistance in the development of this work and for their wonderful company during our time together. Additionally, I am thankful for the support and friendship of Kevin, Cane, Lucas, Vitor, Marcelo, and Jeferson.

I am indebted to the Federal University of Santa Catarina and Technische Hochschule Ingolstadt, along with their esteemed professors, whose contributions made this work possible.

I must also acknowledge the invaluable facilities provided by the CARRISMA institute and express my gratitude for the opportunities enabled by AWARE program to make part of my thesis in Germany.

Finally, I extend my heartfelt thanks to DAAD and FEESC for their financial support, without which this work would not have been possible.

"Whatever tomorrow brings, I'll be there With open arms and open eyes."
(Incubus,1999)

ABSTRACT

This research was driven by the growing demand for parameter estimation methods in automated driving vehicles, aiming for economically viable applications. In order to achieve a reliable parameter estimation it was implemented a 10 Degree of Freedom (DoF) twin track vehicle dynamic model in Python language using modules that represent the vehicle systems powertrain, chassis, suspension, steering, brakes and tires. This model was compared with a virtual solution from "IPG CarMarker" software using data gauged from a BMW M8 Competition in CARISSMA - Institute Automated Driving (C-IAD) at Technische Hochschule Ingolstadt (THI). Additionally, optimization methods were employed for parameters with lower reliability in traditional measurements. Specific maneuvers were conducted to isolate parameter influences on vehicle dynamics, evaluating longitudinal, lateral, and combined behaviors through standardized tests including acceleration-rolling-brake, step steer, and double lane change maneuvers as per ISO 3888-2 norm. The vehicle model yielded coherent results across various aspects, exhibiting synchrony in gear changes, powertrain responses, and brake torque values compared to the base model. In longitudinal tests, pitch values fell within expected ranges, with trends aligning closely with respective throttle and brake inputs. Step steer tests revealed discernible differences in forces between inner and outer tires owing to slip angle variance. Lane change maneuvers served to validate roll angle predictions, showcasing higher values attributable to the model's simplifications, such as the absence of anti-roll bars. Further optimizations were pursued in the powertrain module using genetic algorithms to fine-tune inertial parameters, resulting in noteworthy enhancements in vehicle longitudinal speed, particularly at velocities exceeding 10 m/s.

Keywords: Parameter estimation. Vehicle Dynamic. Vehicle Testing.

RESUMO

Esta pesquisa foi impulsionada pela crescente demanda por métodos de estimação de parâmetros em veículos de condução automatizada, visando aplicações economicamente viáveis. Para obter uma estimativa confiável dos parâmetros foi implementado um modelo dinâmica veicular com 10 DoF em Python, usando módulos que representam os sistemas do veículo: trem de força, chassi, suspensão, direção, freios e pneus. Este modelo foi comparado com uma *software* comercial virtual "CarMarker"utilizando dados aferidos de um BMW M8 Competition no C-IAD em THI. Além disso, métodos de otimização foram empregados para parâmetros com menor confiabilidade em medições tradicionais. Manobras específicas foram realizadas para isolar influências de parâmetros na dinâmica do veículo, avaliando comportamentos longitudinais, laterais e combinados através de testes padronizados, incluindo aceleração-rolamento-freio, *step steer* e teste do alce de acordo com a norma ISO 3888-2. O modelo do veículo produziu resultados coerentes em vários aspectos, exibindo sincronia nas mudanças de marcha, respostas próximas a referência em termos de torque para trem de força e freio. Em testes longitudinais, os valores de inclinação ficaram dentro dos intervalos esperados, com tendências alinhadas estreitamente com as respectivas ações do acelerador e do freio. Os testes de direção escalonada revelaram diferenças perceptíveis nas forças entre os pneus internos e externos devido à variação do ângulo de deriva. As manobras de mudança de faixa serviram para validar as previsões do ângulo de rolagem, apresentando valores mais elevados atribuíveis às simplificações do modelo, como a ausência de barras estabilizadoras. Otimizações adicionais foram buscadas no módulo do trem de força usando algoritmos genéticos para ajustar os parâmetros inerciais, resultando em melhorias consideráveis na velocidade longitudinal do veículo, especialmente em velocidades superiores a $10m/s$.

Palavras-chave: Estimativa de parâmetros. Dinâmica veicular. Teste de veículo.

RESUMO EXPANDIDO

INTRODUÇÃO

Atualmente, todos os carros à venda possuem diversos recursos de segurança devido à crescente preocupação com a segurança dos passageiros, impulsionada por requisitos regulatórios e pressões do mercado. Uma tecnologia promissora na indústria automotiva é a condução automatizada, que pode substituir o condutor humano por um sistema inteligente. Neste contexto, os modelos de dinâmica veicular são imprescindíveis para avaliar diversos aspectos do comportamento do veículo por meio de simulações. Estes são aplicados nas etapas de design e teste de sistemas veiculares, oferecendo simulações de manobras sob parâmetros e condições predefinidos, o que permite reduzir o tempo de desenvolvimento e ajustar produtos de forma econômica e segura. No entanto, recursos e instalações necessárias para avaliar esses modelos, como unidades de medição inercial, bancadas de medição de inércia e túneis de vento, são caras e requerem técnicos especializados. Além disso, alguns parâmetros precisam ser ajustados para condições reais de estrada, o que pode aumentar os custos e atrasar o lançamento dos projetos. Portanto, um processo de estimativa de parâmetros de forma sistemática contribui para testes mais eficazes e barato. Isso possibilita a investigação de diferentes variáveis, como faixa de velocidade, tipos de estrada e condições ambientais, entre outros cenários de teste. Esta dissertação se propõe a adotar uma abordagem sistemática para a estimativa de parâmetros usando um conceito de otimização. Para isso, um modelo de veículo de duas faixas com 10 graus de liberdade foi desenvolvido e integrado com um método de otimização genética aplicado a parâmetros do modelo. A abordagem foi validada por meio de simulações virtuais de manobras como aceleração e frenagem, esterçamento constante e troca de faixa dupla usando como referência o modelo do IPG CarMaker (CM).

OBJETIVOS

Esta tese tem como objetivo desenvolver e testar uma metodologia rápida para estimar parâmetros de modelos de dinâmica veicular, capazes de prever o comportamento do carro em manobras como aceleração, frenagem e curvas. O objetivo é fornecer dados em tempo real permitindo os testes de veículos com condução automatizada. Para alcançar esse objetivo, deve-se escolher um modelo de veículo que forneça resultados representativos em termos de aceleração longitudinal e lateral, além de momentos de arfagem, guinada e rolagem. As saídas serão calculadas com base nas entradas pedal de aceleração, pedal de freio e posição do volante. Propõe-se a separação do modelo em módulos, representando subsistemas como: pneus, suspensão, direção, trem de força, freios e chassi. Testes virtuais serão realizados para avaliar a credibilidade do modelo. Com os resultados obtidos, será realizada uma metodologia sistemática de estimativa de parâmetros.

METODOLOGIA

O processo começa com a identificação de parâmetros do modelo, que envolve a estimativa e medição dos parâmetros necessários para avaliar o modelo implementado. Para estimar os parâmetros de um veículo matematicamente, é necessário usar um modelo representativo que considere os aspectos avaliados. Para isso, foi implementada uma rotina de

modelo de veículo com "pista dupla"usando a linguagem Python. O modelo possui 10 graus de liberdade, sendo utilizado para estudar o comportamento do veículo nas direções longitudinal, lateral e vertical, além das rotações nessas direções e da velocidade de rotação de cada roda. No modelo desenvolvido, suspensão das rodas é conectada ao chassi por molas e amortecedores, onde a interação de forças aplicadas. O chassi é considerado um corpo rígido com 6 graus de liberdade, e assume-se que as rodas só se movem verticalmente em relação ao chassi, sem representar a influência de parâmetros cinemáticos como o ângulo de cambagem na suspensão. No entanto, estas considerações são suficientes para investigações iniciais e para simuladores de modelos básicos de veículos. O modelo desenvolvido foi separado em módulos: Chassis, direção, pneus, suspensão, visando facilitar a implementação e aferir modularidade a diferentes analises. Para validar o modelo implementado, são necessários testes virtuais e reais. Medições diretas como entre eixos e bitola aferidos manualmente de forma fácil. Outros como o centro de gravidade são aferidas experimentalmente. Bem como a referência bibliográficas e medições indiretas são usadas para parâmetros com medição mais complexa, como parâmetros dos pneus e inercias rotativas dos componentes do trem de força. As manobras realizadas foram: uma sequência de aceleração, rolagem e frenagem, saindo da inercia até 8 m/s, 18 m/s e 25 m/s, tanto no modelo CarMaker quanto no modelo implementado. A manobra de mudança de faixa dupla foi realizada conforme as recomendações da ISO 3888-2, com velocidades mantidas em 8, 18 e 25 m/s. Passos de esterçamento foram executados a velocidades constantes de 8, 13 e 18 m/s em um percurso circular com diâmetro externo de 45 metros, para avaliar o comportamento dinâmico em rolagem e as acelerações laterais máximas. Na otimização, os valores de componentes de inercia do trem de forca foram avaliados dentro de um intervalo pré-estabelecido. Para enfrentar o desafio da contaminação, a otimização é realizada de forma modular, permitindo uma abordagem sistemática para mitigar problemas potenciais. Utilizam-se algoritmos genéticos (GA) para otimizar os valores de rigidez e inércia em um modelo de veículo. A otimização foi realizada com parâmetros específicos que impactam significativamente o v_x, como inércia da caixa de câmbio, do motor, das rodas e do eixo de transmissão.

RESULTADOS E DISCUSSÃO

Os resultados dinâmicos como deslocamentos, rotações e suas derivadas do modelo implementado foram comparados com o modelo de referência do CarMaker, considerando os mesmos dados de entrada. No primeiro momento, foi feita a validação do módulo de transmissão. Os resultados mostram que a velocidade longitudinal do veículo atinge 14 m/s em 11 segundos, quase idêntica à verificada no IPG CarMaker. Foi realizada uma análise das respostas de aceleração lateral, taxa de guinada, ângulo de rolamento e ângulo de deslizamento dos pneus. Os resultados de validação do modelo de 10 graus de liberdade mostraram uma tendência semelhante entre a simulação e o experimento, com pequenas diferenças na magnitude. Durante o teste de mudanças de faixa, que visa avaliar o comportamento e o desempenho do veículo em manobras laterais rápidas, simulando situações reais como mudanças de faixa de emergência ou manobras evasivas. A análise foca em características de rotação do veículo, como ângulo e taxa de rolagem, e na transferência de carga, que são indicadores importantes da estabilidade e conforto do veículo. Os dados de rolagem dos modelos durante uma mudança de faixa, mostrando tendências semelhantes, especialmente em ângulos de rotação, com o modelo implementado alcançando um máximo de 0,4 radianos e o modelo CarMaker 0,15 radianos, quase três vezes

menos. Esta consistência sugere a possibilidade de ajustar o parâmetro de resistência à rotação para alinhar melhor com o modelo de referência. Bem como, a ausência do efeito da barra estabilizadora na simulação pode ser uma fonte de erro, já que essa barra é crucial para reduzir o ângulo de rotação. Ao considerar as forças nas rodas, observa-se uma forte dependência na direção x com a entrada de torque e uma maior amplificação das forças laterais nas rodas externas do eixo dianteiro devido à transferência de peso. Após a otimização do parâmetro inercial do trem de força, os resultados alcançaram uma velocidade longitudinal de 0 a 10 m/s, com a diferença se tornando quase imperceptível e a desvio máximo, observado em torno de 25 m/s, diminuindo de 3,75 m/s para 1,25 m/s. A validação demonstrou que o modelo pode representar o comportamento dinâmico real do veículo. As diferenças surgem devido à simplificação do modelo, como a desconsideração da barra estabilizadora, flexibilidade do corpo e movimento do centro de rolamento, além da dificuldade do motorista em manter uma velocidade constante durante as manobras de teste.

CONCLUSÃO

Em conclusão, foi desenvolvido um modelo de veículo com 10 graus de liberdade que incluem para o estudo da dinâmica veicular. Este modelo foi validado com manobras padronizadas utilizando o CarMaker, focando nas características longitudinais, laterais e transitórias durante aceleração, frenagem, esterçamento e troca de faixa. O processo de identificação dos parâmetros foi realizado em duas etapas distintas. Inicialmente, foram medidas diretamente todos os parâmetros essenciais do modelo, como a localização do centro de massa, valores de inércia do chassi e dos pneus, e parâmetros da suspensão. Parâmetros além da capacidade imediata de medição, como os do modelo de pneus Pacejka 1989, foram identificados por meio de extensa revisão da literatura. Em seguida, foram realizados testes de validação para avaliar a precisão do modelo e refinar os parâmetros inferidos da literatura existente. Foi realizada uma análise das respostas de aceleração lateral, taxa de guinada, ângulo de rolamento e ângulo de deslizamento dos pneus. Os resultados de validação do modelo de 10 graus de liberdade mostraram uma tendência semelhante entre a simulação e o experimento, com pequenas diferenças na magnitude. Com os resultados obtidos, é possível afirmar que o método pode acelerar a estimativa de parâmetros para futuros desenvolvimentos em veículos com condução automatizada. Contudo, apesar dos avanços no campo da condução automatizada, ainda há desafios significativos relacionados à infraestrutura, custo e maturidade técnica que devem ser superados para alcançar a aplicação comercial generalizada dos sistemas autônomos. Para aprimorar o modelo dinâmico veicular é sugerido o refinamento dos modelos de pneus e suspensão. Embora os modelos de pneus atuais ofereçam precisão, avanços no modelo Pacejka, que consideram fatores como variação de carga normal, empuxo de cambagem, flutuações de temperatura e atrito com a estrada, captam com maior a fidelidade da resposta transitória dos pneus. O modelo de suspensão, que atualmente utiliza molas e amortecedores lineares, pode ser aprimorado com componentes adicionais como barras estabilizadoras e considerações cinemáticas. Para acelerar o progresso e ampliar a aplicabilidade, propõe-se melhorar a modularidade para permitir aprimoramentos simultâneos em vários módulos, adaptar modelos de transmissão para refletir sistemas modernos, explorar técnicas alternativas de modelagem como redes neurais, agilizar a base de código para testes eficientes e expandir a modelagem de pneus para diferentes condições de terreno e fatores como pressão e temperatura.

Palavras-chave: Estimativa de parâmetros. Dinâmica veicular. Teste de veículo.

LIST OF FIGURES

LIST OF TABLES

LIST OF ABBREVIATIONS AND ACRONYMS

ADAS	Advanced Driver-Assistance System
CAN	Controller Area Network
CG	Center of Gravity
C-IAD	CARISSMA - Institute Automated Driving
CM	IPG CarMaker
DoF	Degree of Freedom
DT	Double Track
ECUs	Engine Control Unit
FEM	Finite Element Method
GA	Genetic Algorithm
HIL	Hardware in the Loop
IMU	Inertial Measurement Unit
ISO	International Organization for Standardization
MBS	Multibody Systems
MF	Magic Formula Model
MIL	Model in the Loop
MPC	Model Predictive Control
PID	Proportional–Integral–Derivative
SCIL	Scenario-in-the-Loop
SIL	Software in the Loop
THI	Technische Hochschule Ingolstadt
VIL	Vehicle in the Loop

LIST OF SYMBOLS

γ	Camber angle
σ	Kingpin inclination
r_s	Scrub radios
ϕ	Roll angle
θ	Pitch angle
ψ	Yaw angle
m	Total vehicle mass
m_s	Sprung mass
m_u	Unsprung mass
w	Track width
h	Wheelbase
V_r	Wheel velocity
v_x	Tangential velocity
α	Sideslip angle
μ_x	Longitudinal friction coefficient
μ_p	Peak friction coefficient
F_x	Wheel forces at longitudinal direction
F_y	Wheel forces at lateral direction
M_z	Moment at at the z axis
M_y	Moment at at the y axis
F_z	Wheel forces at vertical direction
k_s	Spring Stiffness
c_s	Damping coefficient
k_t	Tire Stiffness
Δ_{spring}	Spring displacement
ω_d	Damped natural Frequency
ζ	Damping coefficient
V_{crit}	Critical velocity for understeer vehicle
η	Understeer coefficient
i_g	Gear Ratio
i_c	Torque converter ratio
i_D	Differential ratio
f_0	Rolling coefficient
R_r	Rolling resistance
V	Longitudinal speed
C_z	Aerodynamic lift coefficient
ρ	Air density

S	Frontal area
R_a	Aerodynamic resistance
C_x	Aerodynamic drag coefficient
R_i	Residual in least Square
ω_i	Weight associated
x_A	Vehicle state
ω_x	Roll rate
ω_y	Pitch rate
ω_z	Yaw rate
α_m	Angular acceleration
$slip_x$	Longitudinal slip
S_v	Vertical shift
S_h	Horizontal shift
B	Stiffness factor
C	Shape factor
D	Peak factor
E	Curvature factor
δ	Steering angle
v_y	Lateral velocity

CONTENTS

1 INTRODUCTION

Every car on sale today has several safety features. This is a consequence of the increasing concern towards safety on passager car. Regulatory requirements and market pressure are the main drives form development in this field.

One of the capabilities that could be a game changer in the transportation industry is application of a automated driving. This technology is promising due its potential to replace human drive by an intelligent system Feng, Dang, and He [12] and Gao et al. [13]. In order to achieve such a high level of maturity, vehicle models that can predict the vehicle behavior in a large spectrum of scenarios are mandatory. This models play a crucial role in fields such as path planning, image processing, data analysis, low level control of the vehicle and many others.

The aim of modeling is to obtain a mathematical-analytical that is able to represent the vehicle behaviour. As well as evaluate many aspects through simulation environment in order to accurately test how the vehicle will react under many different circumstances [14]. Model-based control design is proven to be a time-saving and cost effective approach that allows move from model creation to simulation, code generation and Hardware in the Loop (HIL) test in a systematic way.[4]

Those models are fundamental in system design and testing, providing simulation for maneuvers under predefined parameters and conditions [44]. Enabling a continuous shortening of product development and tuning with a economic and safer approach.

In order to evaluate this models an advanced test facilities with Inertial Measurement Unit (IMU), vehicle inertia measurement rigs, wind tunnels and drum testing machines are reacquired. These facilities are capable of estimating vehicle positioning, location of vehicle center of gravity, drag coefficient, tire and suspension parameters respectively with high accuracy. However, the application of these facilities is not always feasible and requires skilled technicians to conduct tests. Also, some parameters determined by rig tests need to be adapted to real read condition. All this details lead to costly development process and delay the projects release.

Therefore, speeding up the process of parameter estimation and testing in a more effective way is very appealing. This type of approach enables the investigation of different inputs such speed range, using a variety of road types, speed range, environmental condition, functional constrains and many others that will help to define the test scenarios in automated driving.

Taking that into account, this thesis target a systematic approach for parameter estimation using an optimization concept. For that, a 10 DoF twin track without suspension kinematics vehicle model were implemented and integrated with genetic optimization method applied to several parameter used in the model.

Considering this, the thesis focuses on a systematic method for parameter estima-

tion utilizing an optimization framework. To achieve this, a twin track vehicle model with 10 degrees of freedom DoF, excluding suspension kinematics, was developed. Subsequently, the genetic algorithm optimization method was employed to improve model accuracy through the adjustment of selected parameters.

To validated this approach a series of maneuvers: acceleration and braking, step steer, double lane change were carried out virtually by using IPG CarMaker (CM). Also measurements of relevant coordinates and masses were carried out, for evaluate center of gravity, curvature radius were gauged on THI facilities on a BMW M8 competition for further comparison.

1.1 OBJECTIVE

This thesis aims developing and testing a rapid methodology for estimating parameters of vehicle dynamics models that can predict the car behavior in maneuvers, such as acceleration, braking, and turning. Providing real time data to assist automated driving vehicles testing.

1.1.1 Specific objectives

To achieve this objective a vehicle model with representative results in terms of longitudinal and lateral acceleration, pitch, yaw and roll moments must be choose. The outputs shall be calculated based on throttle, brake and steering wheel position inputs. In order to achieve these objectives, a separation into modules is proposed where subsystems are represented by functions as follow:

- Tire
- Suspension
- Steering
- Powertrain
- Brake
- Chassis

Virtual testing will be carried out to evaluated the credibility of the model. With the results obtained by the implemented model a Systematic parameters estimation method will be performed.

2 LITERATURE REVIEW

This section provide a physical background necessary to understand the principles involved in vehicular dynamic model as well as a a state-of-art in methodologies used for parameter estimation.

2.1 VEHICLE DYNAMICS

Vehicle dynamics is the study of the interaction between a vehicle of any kind and road surface. Understand the vehicle behavior regards to acceleration or braking, ride and turning in a particular maneuver is essential to know how the vehicle will respond to this forces. [18]

2.1.1 Vehicle Coordinates System

To represent the vehicle is necessary to set a standard in the axis orientation. In this work we will assume the coordinates convention by International Organization for Standardization (ISO) as follow in Figure 1. The vehicle motion is referenced with the coordinates:

Figure 1 – ISO Vehicle Axis System.

Source: Author

Where according to Gillespie [18], the following motion variables are assumed.

- x - Forward and on the longitudinal plane of symmetry

- y - Lateral out the right side of the vehicle
- z - Upward with respect to the vehicle
- ϕ - Roll angle about the x axis
- θ - Pitch angle about the axis
- ψ - Yaw angle about the z axis

Occasionally, an additional axis system is required to acknowledge the vehicle position relative and direction to an external reference. In this case an earth-fixed system is used, this axis frequently coincides with vehicle axis at the initial state, but they are independent according to Milliken and Milliken [36].

Once the coordinate system is defined, there still plenty of parameters that play an important role on vehicle dynamics. Starting with the vehicle mass (m), that is usually split in sprung mass (m_s) and unsprung mass (m_u). The unsprung is the portion of the total mass of the vehicle which is not supported by the suspension springs and sprung mass is that portion of the total vehicle weight which is supported by the suspension springs. This includes the chassis, engine, driver, fuel, gearbox, etc [46].

Figure 2 – Frontal View Of Suspension links.

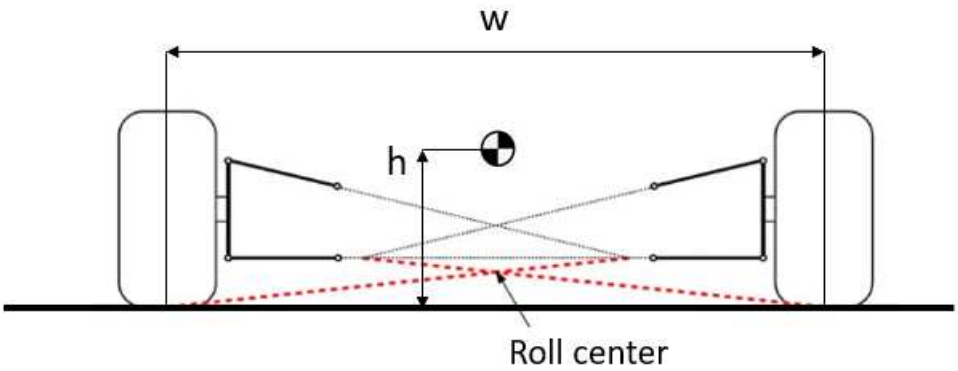

Source: Author

The track width w is defined as the distance form imaginary vertical lines the cross the center of the tire on the frontal view as shown in Figure 2. Thus, a vehicle can have different frontal and a rear track width. At Figure 2 is also shown the center of gravity high h, that is defined as that point about which, if the body were suspended from it, all parts of the body would be in equilibrium i.e. without tendency to rotate [46].

Additionally, the instant center is important to determining several common suspension parameters and can be found by the point of the projected lines from the upper and the lower suspension arm [36].

The roll center height is found by projecting a line from the instant center of the tire-ground contact path through the front view instant center, the procedure is done both sides as Figure 2. When a car corners the centrifugal force at the center of gravity is reacted by the tires and the roll center establishes the force coupling point between m_u and m_s [36].

Note that in the case of a two-axle vehicle the roll center of each suspension can be determined from the characteristics of the relevant suspension only, and that the roll axis can be defined as a line connecting the roll center of the two suspensions [16].

Similarly to the the track width, it is possible to represent the wheelbase as the distance projected on a xz plane between the center of tire contact area of the wheels of the same side and track and the distance projected on a yz plane between the centers of the contact area of the wheels of the same axle [16].

Most vehicle dynamic analyses are based on Newton's second law for transnational and rotational systems. The representation of this is a free-body diagram, where appropriated forces and moments are substituted at contact point with the external reference, along with gravitational forces [18].

Thus, it is possible to evaluate longitudinal, lateral, vertical acceleration as well as Euler angles of the vehicle. For the purpose of understanding the dynamic behavior can be split by systems as follow in the next subsections.

2.1.2 Wheels and Tires

Figure 3 – Tire input.

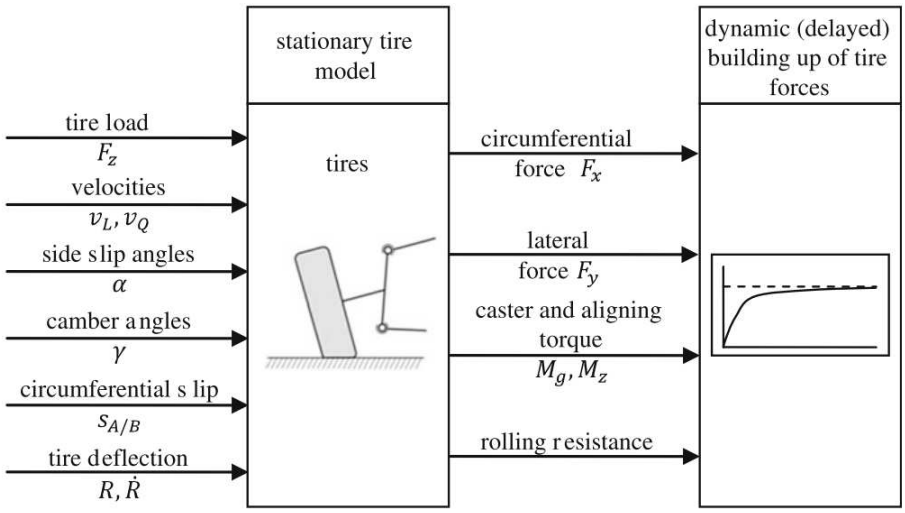

Source: [44]

In order to understand the vehicle behavior is essential know how the forces interact with the ground. The vehicle wheels have to withstand vertical, longitudinal and lateral

forces, as well as move and control the vehicle path [16]. All the given inputs placed in the vehicle will interact with the surrounding through the tire.

Figure 3 represents a stationary model with important inputs for tire integration, such as load, velocities, and slip angles. All these constraints interact with external forces to become the final tire force.

The tire can be compared to an elastic deforming structure with internal damping. Thus, rolling radius will assume a value smaller than the unloaded value, because of the applied vertical force. The forces transmitted between tire and road surface takes place though the tire contact patch. Force components in the longitudinal and lateral directions which are parallel to the road surface are generally transmitted through friction [44].

Hysteresis and adhesion are the mechanisms responsible for friction coupling. Surface adhesion comes from the inter-molecular bonds which exist between the rubber and the aggregate in the road surface, while hysteresis represents an energy loss in the rubber as it deforms when sliding over the aggregate [19].

The longitudinal slip of the tyre is defined as a ratio between slip velocity in contact path divided by forward velocity as follow in Equation (1). Where V_r is wheel velocity and v_x is the tangential velocity. The absolute operation makes this equation work in both acceleration and braking conditions.

$$slip_x = \frac{|V_r - v_x|}{v_x} \tag{1}$$

The lateral slip (α) is defined as the ratio of the lateral velocity $V_{lateral}$ of the contact center and the longitudinal speed v_x as follows in Equation (2)

$$\alpha = -\tan \frac{v_{lateral}}{v_x} \tag{2}$$

The variable tangent α is also known as the lateral slip and the angle as the slip angle. According to Heißing and Ersoy [20], in normal driving conditions the slip angle and the lateral slip can be set to be the same as a good approximation.

Over driving or braking force to a tire that has a certain slip angle, the cornering force reduces, the same applies to the longitudinal force a tire can experiencing a lateral force. By setting the tire at a given slip angle and applying a braking torque, the shape of the curve μ_x (δ) is deeply changed, meanwhile the value in slipping conditions μ_s is almost unchanged, the peak value μ_p decreases to a greater extent [16].

Knowing the slip angles and tire normal forces makes it possible to estimate the lateral force on each wheel. There are several tire models for applications in vehicle models, with ranges of complexity ranges from the simple linear to the very complex nonlinear models, depending on the situation and the application [44].

One of the most widely used tire models is Magic Formula Model (MF) that was developed by Pacjeka and Bakker (1993). The MF tire model is a mathematical description

Figure 4 – Lateral and longitudinal force coefficients as function of longitudinal slip and sideslip angle.

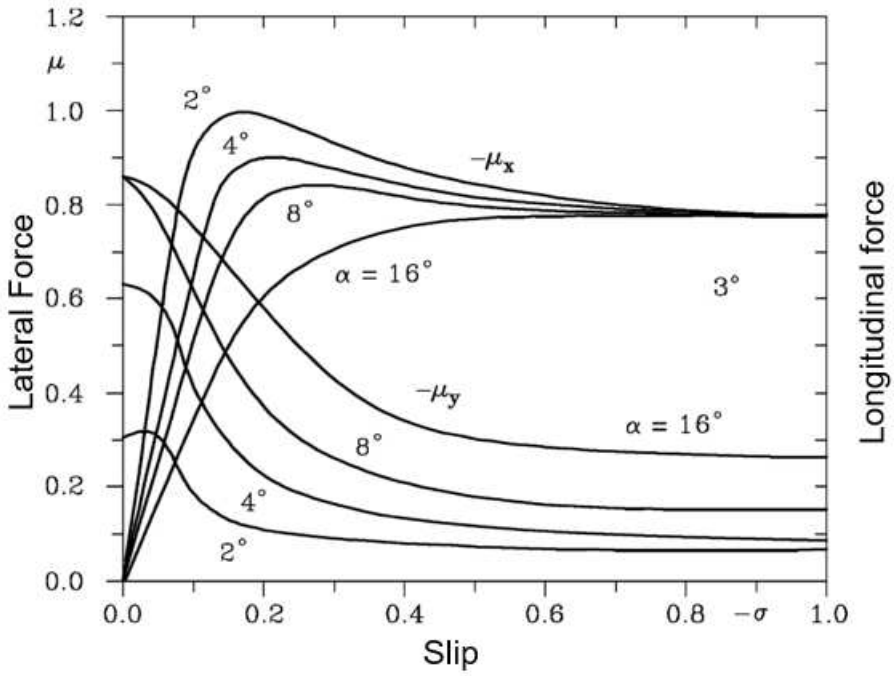

Source: Adapted from Genta [16]

of the input-output relationship of the tire-road contact tested experimentally under quasi-stationary conditions. The tyre is rolled over a road at several loads, orientations and motion conditions [39].

This model calculates the forces F_x, F_y and torques M_z, M_y acting on the tyre at pure and combined slip conditions, using longitudinal and/or lateral slip , wheel camber and the vertical force F_z as input quantities [39].

2.1.3 Suspension System

The work principle of a vehicle suspension is manage the wheel movement and isolate the chassis from surface irregularities. Whereas allow distribution of forces, exchanged by the wheels with the ground. Suspensions is therefore essential for achieving adequate handling and comfort, as well as determining distinctive characteristics of the vehicle [16].

To achieve a good performance in these aspects, usually a defined set of target for suspension motion, than kinematic mechanism represented by rigid beams, spherical joints, bushings and so on is developed. There are many parameters that need to be comprehended to model the suspension behaviour, such as camber, caster, toe, king pin inclination.

Camber is defined using the vehicle frontal view, being the wheel inclination angle

Figure 5 – Camber γ as defined by ISO 612 / DIN 70000.

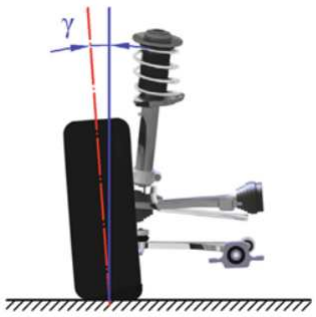

Source: Heißing and Ersoy [20]

relative to a vertical line crossing the center of the wheel as shown in Figure 5. Camber influences lateral dynamics, aligning torque, and suspension tuning [20].

The scrub radius is the distance from the intersection of the steering axis and the roadway to the intersection of the wheel center plane with the roadway. Negative scrub radius creates a steering wheel moment in the proper direction to counteract vehicle yawing Figure 6. The kingpin inclination determines the scrub radius, thereby influencing the steering self-aligning, providing stability when vehicle moves straight forward and a self adjusting when cornering [20, 35].

The kingpin angle also affects tie rod length and caster change [20]. Caster is built into the front suspension to promote straight line stability and to provide feel and self returning action. The ideal caster angle has to be played with Smith [46] and adjusted to car application.

Figure 6 – Kingpin Inclination σ, scrub radius r_s.

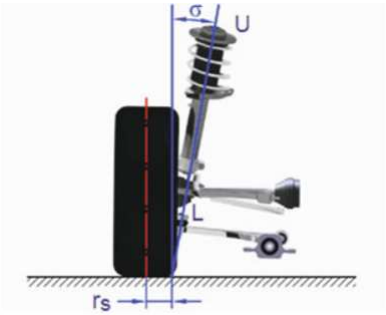

Source: Heißing and Ersoy [20]

Vertical dynamic behavior is a simplification of vehicle body roll and pitch motion and accelerations with the perspective of the vertical wheel force changes, and vibration behavior, that is handled by the suspension system.

Aiming proper ride isolation the essential dynamics can be represented by a quarter car model. This type of model is composed by the sprung mass m_s, spring k_s and a dumper c_s connected to the unsprung mass m_u with stiffness k_t representing the tire, as shown in Figure 7.

Figure 7 – Quarter Car Model.

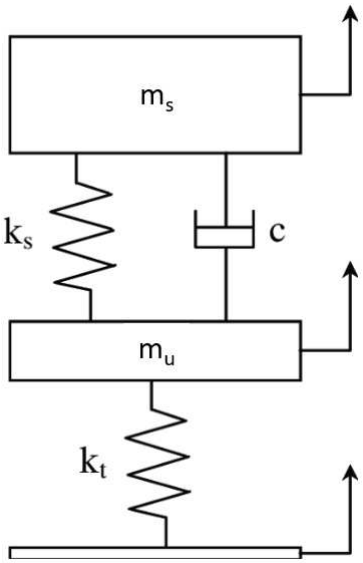

Source: Author

Spring produce a counteracting for when elastically deformed. In general, coil springs have a linear force/displacement curve. Thus, the spring force can be calculated as Equation (3), where k_s is the spring stiffness in (N/m) and Δ_{spring} represent the spring displacement:

$$F_{spring} = k_s \Delta_{spring} \tag{3}$$

Is important to point out that spring ratio is define by vertical load imposed to wheel thorough kinematic mechanism. Thus it depends on type o suspension chosen. Natural frequency and forces are taking into account to define spring and dumper characteristics. The natural frequency Ω_n of this system is given by:

$$\omega_n = \sqrt{\frac{\frac{k_s k_t}{k_s + k_t}}{m_u g}} \tag{4}$$

When damping is present, the resonance occurs at the damped natural frequency ω_d, shown in Equation (5). Shock absorbs are provided to waste the elastic energy stored by the elastic members and to allow the oscillation damping of the vehicle body, avoiding stationary vibration or resonance.[16]

$$\omega_d = \omega_n \sqrt{1 - \zeta^2} \tag{5}$$

where:

$$\zeta = \frac{c_s}{\sqrt{4 k_s m_s}} \tag{6}$$

Other stiffness elements such as anti roll bar or anti dive/squat mechanism can be used to tune response characteristic of the car respective to roll and pitch movements.

Anti roll bar are applied to mitigate this angle amplitudes. During body roll the wheel to the outside the curve is compressed, while the inside wheel becomes extended, limiting in this way the angle of roll [16]. Anti-dive and anti-squat are mechanism, used to limit the pitch by using the inclination of the suspension arms to handle part of the load transfer between axles [9].

2.1.4 Steering System

In dynamic vehicle behavior the steering system has an important role. The vehicle stability and maneuverability depends on steering system characteristics [37]. Most passenger vehicles uses the rack and pinion steering system. This system consists of the rack, two tie rods and two steering arms of the wheel knuckle. Steering mechanisms are restricted positioning due to engine compartment, suspension linkages and other vehicular systems.

For the vehicle inner and outer wheel in steady-state cornering there is a kinematic relation called the Ackermann condition, where δ_0 is the steer angle of the outer wheel, δ_i is the inner wheel steer angle, w is the track and l is the wheelbase of the vehicle [37]. This condition means that the inner wheel has a bigger steer angle than the outer wheel, because is closer to the center of rotation as exemplified at Figure 8.

This mean that when the vehicle is following a curved path, the inside front wheel will be steered to greater angle than the outside. So that both can follow their individual radius without sliding. No single intersection point will result in true Ackermann steering over the whole range, but by moving the intersect point [46].

For the sake of simplification, some models can considered the same steering angle in both wheel. This is done when model not take cinematic into account. According to Genta and Morello [15], the steering angle may be considered a variable, linked by a an equation expressing the compliance of the steering system to the angle at the steering wheel δ given by an input.

The differences between understeer and oversteer become evident in how steering adjustments are required at varying speeds. In an understeering vehicle, you need to increase the steering angle as speed increases to maintain a constant turning radius. This is because the vehicle tends to continue straight ahead rather than turning as much as

Figure 8 – Ackermann geometry.

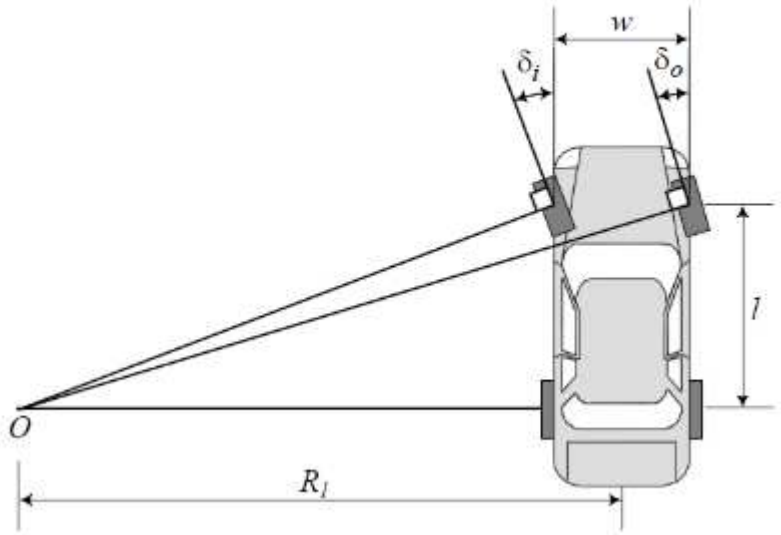

Source: Moldovanu, Csato, and Bagameri [37]

desired. On the other hand, for an oversteering vehicle, you must reduce the steering angle or countersteer at higher speeds to maintain a constant turning radius. The rear end of the vehicle tends to swing out, requiring adjustments to stabilize the car and prevent excessive turning. Figure 9 is shown the relation between the lateral acceleration and the steering angle under oversteering and underteering behaviors.

Figure 9 – Steer angle versus lateral acceleration at constant path curvature.

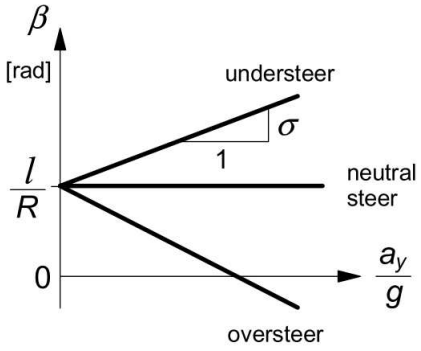

Source: Pacejka [39]

The V_{crit} critical velocity is the point which the oversteering vehicle can became unstable. Steer angle changes sign when for an oversteered car the speed increases beyond the critical speed that is expressed by the Equation (7):

$$Vcrit = \sqrt{\frac{gl}{\eta}},\ (\eta < 0) \tag{7}$$

It is important denote that η Understeer Coefficient has relationship with vertical axle loads that occur at stand-still and thus represent the mass distribution of the vehicle. Changes of these loads due to aerodynamic down forces and load transfer at braking or driving, tire pressure/temperature are not considered in this equation and can change significantly the car behavior [36, 39, 46]. Understeer can be considered beneficial in sports cars and some racing applications, nevertheless in passenger car this characteristic is usually avoid due the instability under high speeds that may cause accidents.

2.1.5 Powertrain

To describe the longitudinal performance of the vehicle, the main information that is required is a description of the torque applied to the wheels over time and/or as a function of speed. The powertrain is composed by a propulsion system, that is connected to the wheel. The Figure 10 represents an schematic propulsion system. The input parameters are the accelerator pedal, gear & clutch, and brake pedal represented in Figure 10.

The signal to the engine to provide a torque to the wheel came from the throttle well as an engine rpm inputs. This torque goes through clutch or torque converter to a gearbox. Inside the gearbox, engine speed and engine torque are converted. The subsequent differential gear distributes the torque equally onto the right and left output shaft [44]. In this path some the torque deliver at the wheel is reduced by the amount required to accelerate the inertial rotation components.

Figure 10 – Powertrain Model.

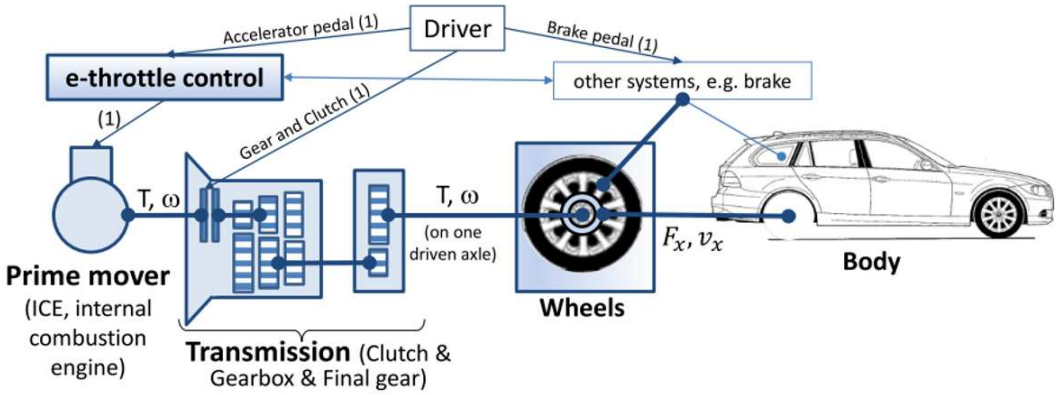

Source: Bonnick [3]

The choice of gear in internal combustion engines relies on factors such as engine RPM and throttle position. Optimal selection is crucial for transferring the intended torque to the wheels effectively. The most common transmission use planetary gears and torque converter, due its smooth power delivery and wide range of operation. As a compromise part of the power is lost in the torque converter fluid.

Alternatively developments in mechatronics has enabled to leave out the torque converter and the planetary gears resulting in what often meant with powershifting transmissions[3]. In practice, one can often manage with 2 clutches, and instead select different paths through gear wheels with synchronisers. Which leads to that a vehicle with converter have typically good acceleration performance and drive-ability [3].

The ultimate output of the transmission reveals itself as the final transmission ratio. This ratio is contingent upon the interplay of gear ratios, torque converter ratios, and differential ratios. Mathematically expressing this relationship:

$$Final\ ratio = i_g * i_c * i_D \tag{8}$$

where:

- i_g - gear ratio.
- i_c - torque converter ratio.
- i_D - differential ratio.

Gear ratio i_g are depended on the gear selected. The gear itself are chosen by a control system depending on engine rpm, vehicle speed and some control system also may include other parameters such as road slope. Torque converter ratio i_c is calculated using the rotational rates between the engine and the driveshaft as in the Figure 11, where a typical curve of i_g for a given speed ratio is presented. It is also important to note that achieving a higher gain in torque often results in a trade-off with energy efficiency. As illustrated in Figure 11, when torque amplification is high, efficiency tends to be lower. Efficiency improves until it reaches a peak value, after which the clutch is locked.

As previously noted, the choice of gear will impact the gear ratio. This can be done by using the engine speed and throttle position.

2.1.6 Resistance forces

The main resistance forces in a vehicle in a flat road is the rolling resistance and the aerodynamic drag resistance. To estimate properly the rolling resistance is used the Equation (9), where the aerodynamics lift is considered. The assumptions of rolling coefficient f_0 is the same on all for wheel and aerodynamic lift is take into account [15].

Tire rolling resistance coefficient R_r is dependent on the friction coefficient and tire load. Assuming that the rolling coefficient f is the same for all wheels, the Equation (9) can be used to estimated the rolling resistance with aerodynamic lift:

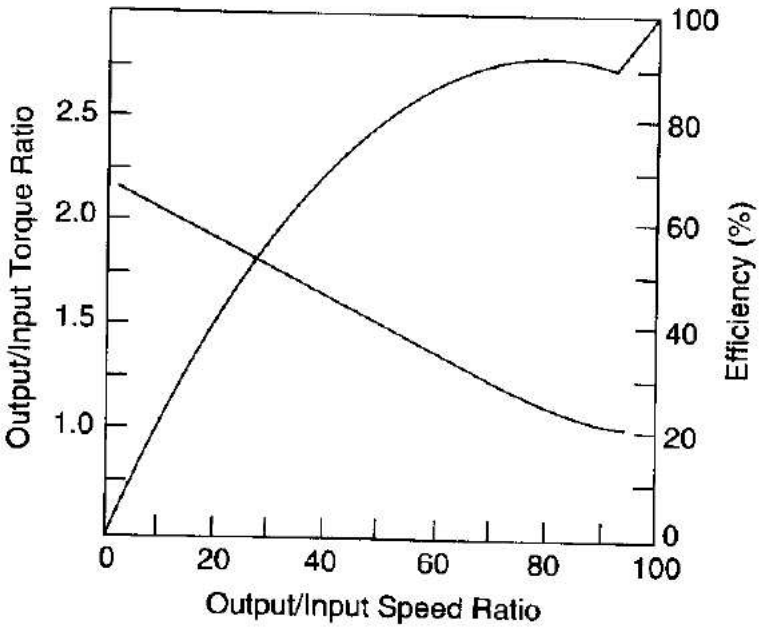

Figure 11 – Output ratio converter

Source: [18]

$$R_r = (f_0 + KV^2)\Sigma F_{z1} = [mgcos(\alpha) - \frac{1}{2}\rho V S C_z]\ (f_0 + KV^2) \tag{9}$$

For the aerodynamics is used Equation (10), where ρ is air density and S is the frontal area of the vehicle. The aerodynamic resistance raises with increasing speed, the importance of the former grows; at a given value of the speed aerodynamic drag becomes more important than rolling resistance.[15]

$$R_a = \frac{1}{2}\rho V^2 S C_x \tag{10}$$

Aerodynamics forces are also important to determined the maximum lateral acceleration, particularly in race car application due the increasing on vertical load at high speeds [36].

2.1.7 Brake system

Friction brakes are used to decelerate and stop the vehicle. They can apply almost unlimited force, as they can lock the wheels in most driving situations. Although the vehicle deceleration is limited often by the tire-road friction.

However, the friction brakes are used for a long time the brake lining will start to fade, lose friction capacity due to high temperature caused be oxidation or melting of the friction surfaces.[3]. The heated fluid with water vapor boils, the formation of water

vapor in the lines leads to system failure by losing the ability to transmit pressure by compression. [34]

The basic design of a passenger car brake system is a hydraulic system. Here, the brake pedal pushes a piston, which causes a hydraulic pressure. The hydraulic pressure is then connected to brake calipers at each wheel, so that a piston at brake calipers press the disc brake dissipation the car's kinematic energy with the pad-disc friction.

There are high complexity brake models, for developing and testing brake system. Although, for vehicle models this system can be simplified using only the brake pedal (input) position and wheel torque (output) for determine the load transfer based on position, velocities, acceleration.

2.2 VEHICLE MODELS

In order to predict the vehicle behavior in the next time step usually a mathematical model is applied to describe the dynamic interaction of the vehicle loading under a specific conditions. In the contest of parameter estimation problems, theses models are useful tools to proper tune and validate the results with agility and efficiency.

In a broad review of vehicle models, two approaches can be highlighted, the physics based models and empirical ones [28]. The mathematical model must be as detailed as possible to represent accurately and completely all the essential properties of the vehicle system. On the other hand, the model must be as simple as possible to allow efficient and fast simulations.[28]

According to Schramm, Hiller, and Bardini [44] vehicle dynamical models can be classified, depending on the required application, different complexity level can be adopted.

Figure 12 displays some of the most commonly applied models in current research and practice. This wide range of applications goes across various industries and fields. These models are useful in vehicle components development, Advanced Driver-Assistance System (ADAS) developing and testing in a wide range of simulated environments, as well as racing simulation and many others. To summarise the applicability of some types of vehicle models the Table 3, where a comparison of single track, Double Track (DT) and multi-body are made.

Table 3 – Vehicle Model Comparison.

Vehicle Dynamic Model	**Kinematics**	**HIL**	**Computational Cost**
Bicycle	Indirectly	Most Used	Low
DT Without Kinematic	Indirectly	Possible	Medium
DT With Kinematic	Directly	Possible	High
Multi Body	Directly	Not Feasible	Extremely High

Source: Author

Figure 12 – Overview of vehicle models.

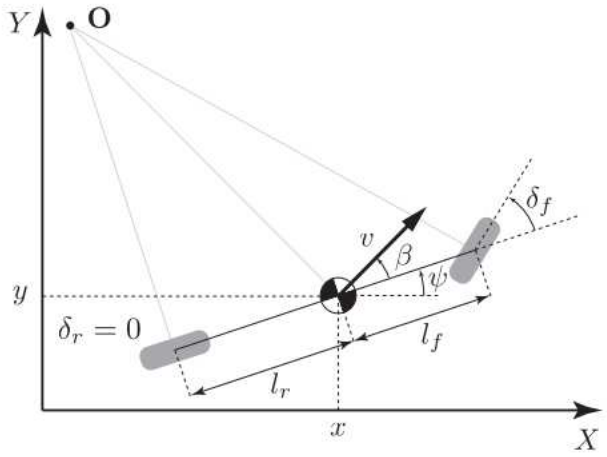

(a) Bicycle model

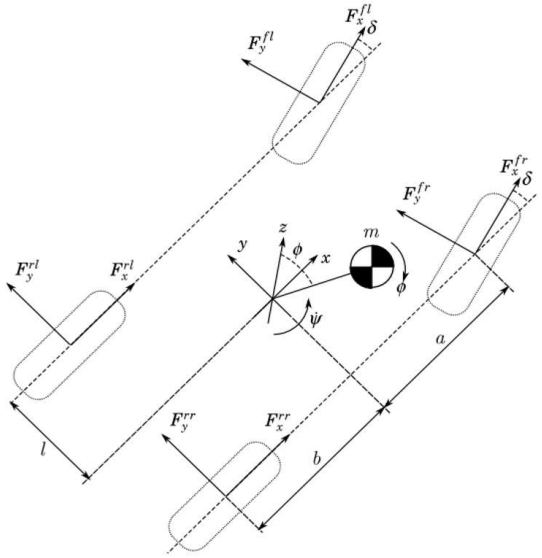

(b) Double track model

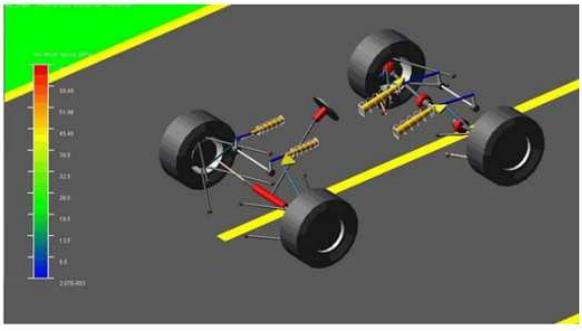

(c) Multi-body model

Source: a)Kong et al. [31], b)Castro, Rill, and Weber [8] and c)Kolera-Gokula [30]

Figure 12a represents the most straightforward approach to vehicle modeling, commonly referred as single track or bicycle model. Due to its simplicity in modeling and parameter estimation effort, the single-track model is one of the most used models [44]. Although, there are many information lost in this type of model due the lack DoF and some simplification such:

- Neglecting the effect of the steering system, assuming that front wheel have the same steer angle and the rear wheels have no steer.
- Left and right tire slip angles are equal, the front-wheel steering angle is small, and the lateral forces are proportional to the tire slip angles.
- The effect of aerodynamics and the load transfer between the left tire and the right tire is neglected.
- The vehicle is assumed to only move in the yaw plane, neglecting the effect of suspension, so the vertical displacement, the pitch angle, and the roll angle are considered to be zero.
- The pneumatic trail and the aligning torque resulting from the slip angle of the tire will be neglected.
- The wheel-load distribution between front and rear axle is assumed to be constant.

This type of approach is used by Kong et al. [31] and their study delves into the application of kinematic and dynamic vehicle models for model-based control design in the context of autonomous driving. The research involves analyzing prediction errors using statistics based on experimental data, with a specific focus on the impact of discretization on forecast error. The findings from this analysis are leveraged to guide the development of a controller for autonomous vehicles Model Predictive Control (MPC) and a simplified kinematic bicycle model.

This model is highlighted for its computational efficiency compared to existing methods reliant on detailed tire models, especially in scenarios where such models may become singular, such as low vehicle speeds were division by zero may occur. Experimental results underscore the efficacy of this proposed approach across various speeds on winding roads Kong et al. [31].

A comparative assessment between the kinematic bicycle model and the dynamic bicycle model is conducted to inform the design of an MPC. Notably, the study indicates that the kinematic model, discretized at $200ms$, performs comparably well to a dynamic model discretized at $100ms$. The kinematic model is more suitable for low-speed scenarios where tire forces can be neglected, assuming no tire slip and that the vehicle follows the trajectory set by the steering angle. In contrast, the dynamic bicycle model accounts for effects like skidding and slipping, which are evident at higher speeds.

While existing MPC approaches for vehicle control employ higher fidelity models involving tire and road interaction, the type of approach stands out for its lower computational demands and adaptability to a broad range of vehicle speeds, including zero speed. Experimental validations of Jeon et al. [27] demonstrate the effectiveness of the proposed controller in diverse speed scenarios, including stop-and-go situations.

Similar conclusion were made by Chen, Danielson, and Iezawa [9] While running a comparison between dynamic bicycle model, 8 DoF vehicle model and 14 DoF vehicle model as a MPC to tracking straight line and circles. It was pointed out that the bicycle controller can successfully navigate a vehicle along the given path and calculates the optimal steering sequences faster; therefore, it is suitable for a possible physical implementation with real-time requirements. These results shown that for some application such as tracking simple models such bicycle models can be suited even without the lack details derided from the simplification made.

Effectively managing extreme maneuvers requires an enhanced modeling approach to capture vehicle lateral dynamics, yaw dynamics, and the interplay between yaw and roll induced by lateral load transfer. Higher-order vehicle model, commonly seen in studies focusing on vehicle rollover scenarios. One such model is the 14 DoF configuration, which incorporates detailed suspension modeling at each corner. The 14 DoF model offers the capability to anticipate vehicle pitch and heave motions, providing a more comprehensive understanding of the vehicle's dynamic behavior.

Within the 14 degrees of freedom (DoF), a distinction can be made between models with kinematics and without kinematics. The former involves the absence of kinematic wheel suspension modeling, where the wheels are directly linked to the vehicle chassis through applied spring and damper forces. In this configuration, it is assumed that the wheel center can only move relative to the chassis and perpendicular to the road. Consequently, this model lacks the capability to explore factors like camber or other spatial wheel motions [44].

Meanwhile, the model with kinematics, incorporates detailed front and rear axle suspensions to allow for spatial motion. This inclusion introduces interference with the kinematics based on the type of suspension employed. Notably, this model enables the estimation of camber and caster, providing a more comprehensive analysis of the vehicle's dynamic behavior.

Setiawan, Safarudin, and Singh [45] used the twin 14 DoF track model to validate with experimental data the performance, ride, and handling of four wheel vehicles. The model representation is shown in Figure 13 with the 14 DoF. The vehicle is model as a rigid body with translation on longitudinal, vertical and lateral directions. Leaving three angular DoF consisting of vertical, roll and pitch motion for the rigid body. Tires are assumed to having contact with the ground all the time and ride is represented by vehicle body connected to four wheels by the spring and damper at each corner, representing 8

DoF.

The vehicle model was validated through instrumented vehicle tests, covering aspects like lateral acceleration, yaw rate, roll angle, and tire slip angle responses. The comparison between simulation and experimentation revealed a consistent trend, with slight variations in magnitude. These differences were attributed to simplifications in the model, such as the absence of an antiroll bar, and the neglected of roll center movement.

Figure 13 – 14 DoF Vehicle.

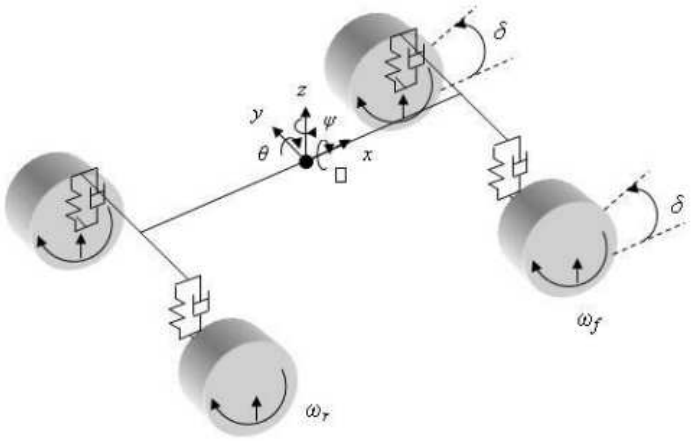

Source: Setiawan, Safarudin, and Singh [45]

Ahmed and Saleh Alshandoli [2] employed the 14 degrees of freedom (DoF) model to develop and deploy a control system aimed at improving lateral stability and vehicle handling. This system utilized two control methods, namely fuzzy Proportional–Integral–Derivative (PID) control theory and a neural network controller. An analysis of the performance and output of the implemented control systems demonstrated the effectiveness of the proposed controllers.

Other like Gennip [14], Chen, Danielson, and Iezawa [9] and [50] used the 14 DoF model to performance analysis and vehicle state prediction and have accomplish satisfactory results in terms of Euler angles prediction and path prediction.

More detailed simulated can take every component into account, using method like Multibody Systems (MBS) presented at Figure 12c and even Finite Element Method (FEM) to calculate load in components to better design them. Although, these type of vehicle modelling proves to be time consuming for real time applications.

They are usually applied in different early stages of the development and can be helpful to estimated some preliminary inputs such as components mass and inertia with a great level of approximation. Also according to Ozcan and Ersoy [38] the FEM can be applied:

- Modal Analysis.

- Temporary Dynamic Analysis (Studies on issues such as physical displacement and velocity of the system in response to events).
- Bending Analysis (Bending cases and post-bending issues are studied due to the carried loads).
- Fatigue analysis.

Nevertheless, for real time data and HIL MBS concept are not a feasible choice in most cases, because extensive use of sensors and long time run and validate simulation with this complexity.

According to Gao et al. [13] research efforts have explored high-order nonlinear vehicle models to study handling limits, but the computational demands often surpass on-board processing capabilities.

A notable strategy highlighted by Gao et al. [13] involves the deliberate selection of simplified and low-order vehicle models based on specific working conditions. By tailoring the complexity of the model to the demands of the task at hand, researchers can achieve a significant reduction in computational overhead. This approach not only streamlines the computational process but also contributes to the overall efficiency of motion planning systems, making them more adaptable and responsive to varying operational scenarios.

In the pursuit of flexibility for individual subsystems, Karl Popp [28] recommendation of decomposing the system in a modular way remains a cornerstone of contemporary research. This approach involves breaking down the overall system into discrete, independently manageable subsystems. The modular structure allows for focused optimization of individual components, facilitating easier integration, maintenance, and adaptability to diverse operational contexts.

To properly model the vehicle, it is necessary to measure and estimate important parameters of the vehicle, as well as define the aspects of interest to better choose the type of model adopted. This holistic approach ensures a comprehensive understanding of the vehicle's intricacies, enabling more effective modular decomposition and subsequent optimization of each subsystem for enhanced overall performance of the vehicle model.

2.2.1 Parameter Estimation

Certain parameters, such as wheelbase and front and rear track widths, can be measured directly or obtained from manufacturer specifications. However, these alone are inadequate for a comprehensive description of vehicle behavior. To create a model that accurately represents the vehicle, additional tests and calculations are required to determine a wide range of vehicle parameters Schedlinski and Link [43]. The parameters listed in Table 4 serve as examples of some of the most crucial ones, and their significance may vary depending on the chosen model type.

Table 4 – Estimated Parameters.

Symbol	**Parameter**	**Unit**	**Applied model**
cx	Longitudinal Tire Stiffness	**-**	Tire
cy	Lateral Tire Stiffness	-	Tire
μ_x	Road Friction Coefficient	-	Tire
μ_y	Road Friction Coefficient	-	Tire
bx	Longitudinal Tire Stiffness	-	Tire
by	Longitudinal Tire Stiffness	-	Tire
cr	Tire Stiffness (vertical)	N/m	Tire
k_s	Spring Stiffness	N/m	Tire Suspension
anti roll	Anti roll Stiffness (front, rear)	N/m	Tire Suspension
f_{dumper}	Suspension damping rate (front, rear)	Ns/m	Suspension
K_{ras}	Spring rate at pin joint between M_s and M_u	N/m	Suspension
$Ktsf$	Auxiliary torsion roll stiffness front axle	N/m	Suspension
K_tsr	Auxiliary torsion roll stiffness rear axle	N/m	Suspension
K_zt	Vertical Spring rate of the tire	N/m	Suspension
m_u	unsprung-mass	kg	Suspension Chassis
Cd	Air drag coefficient	-	Powertrain
I_{engine}	Engine inertia	kg m^2	Powertrain
r_{dyn}	Dynamic radius of the tire	m	Chassis
I_{wheel}	wheel inertia	kg m^2	Powertrain
I_{uf}	Inertia for unsprung mass about x-axis	kg m^2	Chassis
I_{ur}	Inertia unsprung mass about x-axis (rear)	kg m^2	Chassis
I_{phi_s}	Moment of inertia for sprung mass in roll	kg m^2	Chassis
I_{y_s}	Moment of inertia for sprung mass in pitch	kg m^2	Chassis
I_z	Moment of inertia for sprung mass in yaw	kg m^2	Chassis
I_{xz_s}	Moment of inertia cross product	kg m^2	Chassis
I_{dshaft}	Driveshaft inertia	kg m^2	Powertrain
I_{clutch}	Clutch inertia	kg m^2	Powertrain

Source: Author

The identification and consideration of crucial vehicle parameters play a crucial role in the comprehensive modeling of a vehicle. Specifically, the inertia of the vehicle stands out as a key parameter due to its significant impact on the dynamic behavior and maneuverability of the vehicle.

In the parameter estimation process, isolating specific components of inertia becomes essential for a understanding of the vehicle's response to various maneuvers. For instance, the pitch inertia is pointed out as a critical parameter. This distinction arises from the recognition that certain maneuvers may predominantly influence pitch angles while eliciting minimal effects on roll and yaw angles. By accurately quantifying and isolating the pitch inertia, models can better capture and predict the vehicle's behavior during maneuvers that primarily involve changes in pitch orientation.

To comprehensively capture the motion behavior of the car, it is essential to consider other significant parameters such as stiffness and damping in each evaluated DoF.

This allows for a complete representation of the motion equations. Alternatively, in a more systematic approach, equivalent values can be estimated, but a full MBS analysis is required to measure all the components of the model individually.

Tire parameters such C_x, C_r can be evaluated utilizing test rigs if the necessary facilities are accessible, or standard values can be employed. It is essential to consistently take into account the specific tire model integrated into the vehicle model.

Similar methodologies can be employed to determine the drag coefficient Cd and road friction coefficient μ_x. For estimating the unsprung and sprung masses, a common initial approximation involves considering one-third of the total vehicle mass divided equally at the four wheel. For greater precision, the mass can be accurately measured using scales, the procedure can be done while measuring the Center of Gravity (CG). The same principle can be applied to powertrain parameters, Where virtual model and test rigs are usually applied to find the dynamic characteristics.

In summary, recognizing the importance of vehicle parameters, particularly inertia, allows for a more sophisticated and precise modeling approach. Isolating specific components ensures that the model accurately reflects the nuanced dynamics of the vehicle, leading to more reliable predictions under diverse operating conditions.

2.3 VEHICLE DYNAMICS FOR AUTOMATED DRIVING TESTING

Compute autonomous driving functions need incorporating diverse traffic conditions, various weather scenarios, and ensuring scalability for effective testing and analysis performance. Model-based control design is proven to be a time-saving and cost effective approach that allows the designer to move directly from model creation to simulation, code generation and HIL test in a systematic fashion. [4]

Currently, the "in-the-loop" concept appears to be the most efficient approach for evaluating the interaction between automated vehicles and the control environment[22]. To thoroughly test vehicle models in challenging scenarios, specialized tools are accessible for each stage of vehicle controller development. Beginning with the fundamental, Model in the Loop (MIL) serves as a conceptual representation of computer programs or control algorithms, facilitating rapid verification and algorithm development [3, 40].

Software in the Loop (SIL) is usually verified for pseudo-code in a form that can be embedded in an actual automotive controller. It allows many scenarios can be verified faster than real time.[40] A more elaborated approach is HIL validates the actual Engine Control Unit (ECUs) design and operating characteristics at the hardware level in a laboratory environment. Vehicle hardware-in-the-loop simulations HIL make the development and validation of advanced driver assistance systems ADAS safer, cheaper, and more manageable [17].

The verification of the completed system is performed at the actual vehicle stage. In the actual vehicle phase, the most reliable verification is possible, including vehicle

dynamic characteristics. If several ECUs are tested, the hardware can also contain the communication channel between them, e.g. a Controller Area Network (CAN) bus and hardware is run with real-time [3].

The subsequent phase involves the utilization of the Scenario-in-the-Loop (SCIL) testing environment, as described by Szalay, Hamar, and Simon [48]. In this setting, the examination extends beyond the physical characteristics of the vehicle to include the testing of its sensors through virtual twin realization. In this case the investigated scenario is simulated and fully or partly realised in parallel [22].

Vehicle in the Loop (VIL))represents the scenario where the vehicle is in motion on an actual surface, and the complete environment is simulated. The vehicle's actuators receive their input signals directly from the traffic simulation software, incorporating the use of sensor spoofing.

While it constitutes a Hardware-in-the-Loop approach, SCIL stands closer to realistic environment simulation. This is attributed to the fact that not only is the vehicle physically present on a real surface, but some elements of traffic control are also physically integrated. In this scenario, the vehicle relies on its own sensors, adapting to the specifics of the traffic situation [41].

VIL technique is emerging to construct and utilize a virtual environment. VIL is a fusion environment of a real testing vehicle in the real-world and a virtual environment. It can reflect vehicle dynamics at the same level as the real-world and save the cost of constructing an external environment for system verification [40].

In Figure 14 are presented the stages in that the in-the-loop techniques are applied according to Soltani [47]. By integrating "in-the-loop" techniques in autonomous vehicle development accelerates the testing and validation process, enhances system robustness, and ultimately contributes to the safer deployment of autonomous vehicles on the road.

A variety of commercial tools are utilized in the "in-the-loop" techniques for the development of autonomous vehicles. Specific tools are dedicated to handling vehicle dynamics interactions, featuring purpose-built and sophisticated models of vehicles, drivers, and scripts for conducting test maneuvers. They are well prepared for parameter changes and often have an interface with Simulink [3]. Some of most used ones are mentioned bellow:

- CARMAKER
- Carla Simulator
- CarSim
- veDYNA
- VI-CarRealTime

Figure 14 – V-model for redundant system control system design.

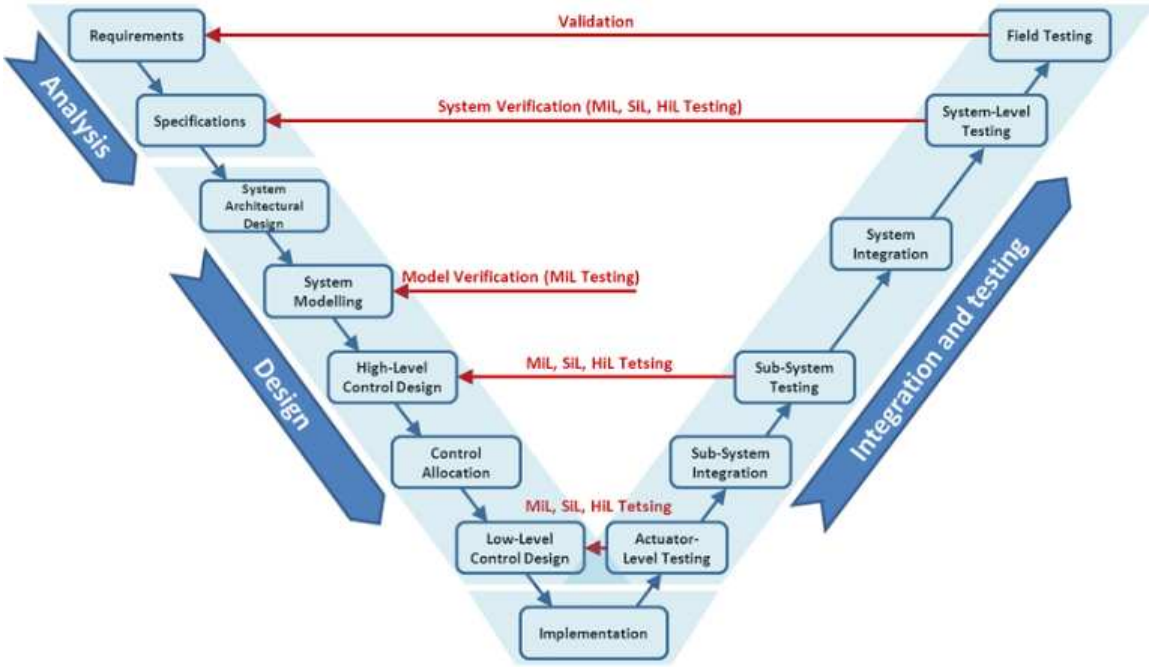

Source: Soltani [47]

- ANSYS VRXPERIENCE

The simulation solution CM by IPG Automotive was specifically designed for the development and seamless testing of cars and light-duty vehicles in all development stages (MIL,SIL,HIL) [6]. It enables the integration of perception, planning, and control algorithms into realistic vehicle dynamics simulations.

Carla simulator stands as an autonomous driving simulator that operates on an open-source framework. CARLA functions as a modular and flexible API, designed to tackle a spectrum of tasks associated with autonomous driving challenges. A primary objective of CARLA is to promote the accessibility and customization of autonomous driving research and development, serving as a tool that can be readily utilized and tailored by users [5].

CarSim provides the most precise, comprehensive, and effective methodologies for simulating the performance of passenger vehicles and light-duty trucks. Having undergone two decades of real-world validation by automotive engineers, CarSim is a popular tool for analyzing vehicle dynamics, creating active controllers, computing a vehicle's performance characteristics, and designing advanced active safety systems CarSim [7].

Each of these tools is designed to fulfill a particular requirement, offering superior performance or better value for the money. It is up to the user to choose the most suitable option for their application.

2.4 MANEUVERS

Driving maneuvers serve as tests to assess the stationary and dynamic behavior of actual vehicles. According to Isermann [23] the primary inputs for these tests include throttle and brake pedal positions, as well as the steering angle δ, while the main outputs are the longitudinal velocity and lateral acceleration.

These inputs have a direct impact on the vehicle's position and attitude. Therefore, standardized driving maneuvers are crucial for analyzing the operational procedures and techniques that drivers use to control and navigate their vehicles safely and efficiently, Tsogas et al. [49].

Established maneuvers contribute to ensuring uniformity and predictability on the road, thereby promoting overall traffic safety. Standard vehicle maneuvers encompass a range of actions, such as turning, changing lanes, merging onto highways, parking, and the execution of various driving techniques.

Adhering to standardized maneuvers is imperative to create a shared understanding among drivers and to comply with traffic regulations and guidelines. These regulations typically define standardized maneuvers, providing a structured and organized framework for safe and orderly traffic flow. The following established procedures are example of standardized vehicle maneuvers for dynamic testing:

- ISO/DIN 4138 [25]: Steady-state circular test procedure (R $<$ 80m); v changed in steps. Measurements of δ, a_Y, $\dot{\psi}, \beta, \varphi, M_H$
- ISO/DIN 7401 [26]: Lateral transient response test methods (steering angle: step, sinusoidal; time response, frequency response).
- ISO 3888-1:2018 [24] Double lane change: Dimensions of the test track are standardized. v_{entry} = 80km/h; $\alpha \cong$ constant or variable. Maximum of v_{entry} can be determined.

Because of the limited speed to change the steering wheel angle, the inputs are actually ramp functions with a speed of about 3.5 to 10 rad/s. Step inputs can be realized with the accelerator pedal or braking pedal within 300 ms.

Figure 15 a) shows a step input (idealized) δ of the steering wheel to generate a transient function of the yaw rate with constant speed v_x. The yaw angle then increases (for slow speeds) linearly and the vehicle corners continuously on a circle with radius R. This maneuver can be used for testing parameter that are more pronounced in lateral dynamic. Is also a good way to identify lateral acceleration response in term of slip angle and validate vehicle path. Roll rate versus lateral acceleration can help estimate inertial parameter one the roll axes is known.

A double lane change like in Figure 15 c) represents an overtaking or evasive maneuver to the left and then to the right. It is a severe test drive for a transient road-

Figure 15 – Standardized Test Maneuvers. a Steering. *b* Lane change. *c* Double lane change (ISO 3888:$l1 = 25m, l2 = 30m, l3 = 25m, l4 = 25m, l5 = 15m; b1, b2, b3$: dependent on vehicle width).

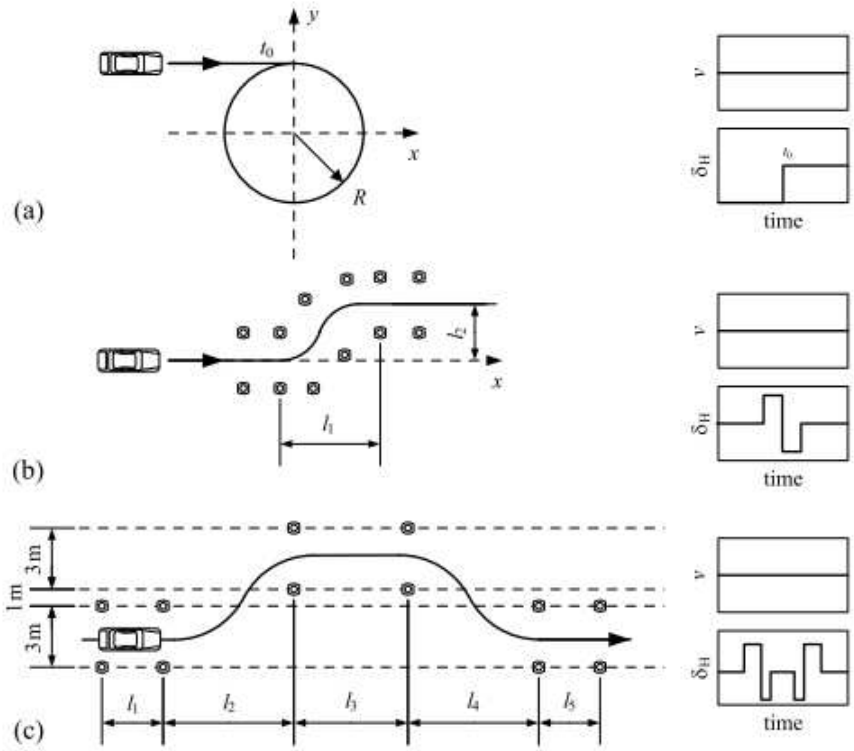

Source: Isermann [23]

holding ability in closed-loop control by the driver and the initial entry speed is v = 80km/h. The throttle position should be as steady as possible [23].

Setiawan, Safarudin, and Singh [45] carried out double lane change test to evaluate the 14 DoF model yaw rate response finding a reasonable fit. A double lane change is a good maneuvers for roll angle parallel between the models to further anti roll bar coefficients tuning.

In automated driving this test maneuvers need input from a control. This sign will enable evaluate in an range of frequency. Some example of non-periodic test signals used are:

- Step function
- Ramp function
- Rectangular pulse
- Double-rectangular pulse
- Double trapezoidal pulse

Other test for harsh condition are extremely hard to reproduce. An feasible approach is to use a test rig. Ružinskas and Sivilevičius [42] compared two tires with same dimensions and different tread pattern and rubber compound under lateral an longitudinal loads. It was found that softer rubber tire had more traction in both longitudinal and lateral tire dynamics than harder rubber. The peak performance of acceleration was twice higher and for braking softer rubber tire had 40%more peak traction. For lateral performance it was 30% [42].

Other non standardized can be adapted according to the goals of the testing maneuvers procedure, facilities capacities and vehicle characteristics.

2.5 OPTIMIZATION METHOD

Achieving optimal performance is an intricate challenge influenced by countless factors. Among these, the selection of appropriate stiffness and inertial parameters plays an important role in determining the vehicle's response to external forces and its overall dynamic behavior. The task of finding an optimal combination of these variables, however, poses a complex, high-dimensional optimization problem.

Numerical optimization deals with the task of finding the values of variables that result in the best possible outcome according to a defined objective function. The objective function encapsulates the variables to be optimized, while constraints may impose limits on the allowable solutions. Traditional methods for parameter tuning may struggle with the intricacies and non-linearities inherent in such systems.

Researchers and practitioners in numerical optimization employ a diverse range of algorithms, from classical methods such as gradient descent and Newton's methods to more advanced techniques like genetic algorithms, simulated annealing, and evolutionary strategies. The choice of algorithm depends on the specific characteristics of the optimization problem at hand.

An optimization problem consists of maximizing or minimizing a one or more functions by systematically choosing input values within an allowed set and computing the value of the functions. For a multi-objective, there are many methods that can be applied. Among then is possible to highlight least square methods, neural networks, genetic algorithm.

Certainly! Here's a revised version:

In response to these challenges, several methods have been developed, including the Least Squares Method, Genetic Algorithm (GA), and Neural Networks. These methods offer different approaches to tackle the optimization problem. Each method has its own strengths and is selected based on the specific requirements of the problem being addressed.

2.5.1 Least Squares Method

The least-squares method is one of the most widely used techniques in statistics, particularly in the context of regression analysis and optimization problems. In regression process, this method is said to be a standard approach for the approximation of sets of equations having more equations than the number of unknowns. The least squares method typically involves solving a system of linear equations or using numerical optimization algorithms to find the values of the model parameters that minimize the sum of squared residuals.

In order to get proper results is essential that the systematic error (biased error) is cancelled. Systematic error arises when a model is unable to capture the underlying relationship between the independent and dependent variables accurately This is done when the parameters are uncorrelated. The method of least squares is generously used in evaluation and regression for parameter estimation for example. A big advantage of the least squares algorithm, however, is that the parameter vector can be determined in one batch calculation and no iterative methods are necessary.[23]

According to Abdi et al. [1] the equation used to find least square is given by the objective function Equation (11):

$$S = \sum_{n=1}^{n=i} w_i R_i^2 = \sum_{n=1}^{n=i} w_i (Y_i - y_i)^2 = \sum_{n=1}^{n=i} w_i (Y_i - f(X_i))^2 \tag{11}$$

where:

- n: Number of data points.
- Y_i: i^{th} input value of the dependent variable.
- y_i: i^{th} computed value of the dependent variable.
- R_i: i^{th} residual, the difference between input and computed values of y for the i^{th} data point.
- X_i (unitalicized): Represents independent variables, scalar if there's one independent variable, or a vector if there are multiple independent variables.
- f: Function expressing the relationship between X and y.
- ω_i : "Weight" associated with the i^{th} data point, further discussed in the next section.

The goal of the least squares method is to find the values of weights that minimize the sum of the squared differences between the observed values and the predicted ones. This minimization process is typically done using mathematical techniques such as calculus or optimization algorithms. Minimizing Equation (11) ensures that the model provides the best fit to the data in terms of total squared error.

2.5.2 Neural Network

Neural network as know as Machine-learning approaches have the advantage of adopting nearly every system's behavior, where this is sufficiently represented in training data Hermansdorfer et al. [21]. The neural network mimics the mechanism of the brain, using a network connection of nodes in the place of neurons and the connection between the "neurons" is made by weight values [10].

Empirical approach relies on measurements conducted with prototypes of components or vehicles. These measurements are then processed using identification methods, leading to the development of a mathematical model. In this process, the system under examination is stimulated with well-defined test signals, and the resulting responses are recorded. By analyzing the input-output relationship, the parameters of the mathematical model are identified, taking into account prior knowledge about the system's structure. This methodology is referred to as parametric identification Karl Popp [28].

The neural network method takes input data, which is usually a set of features or attributes. Each feature is represented by a node in the input layer as shown in Figure 16:

Figure 16 – Neural Networks

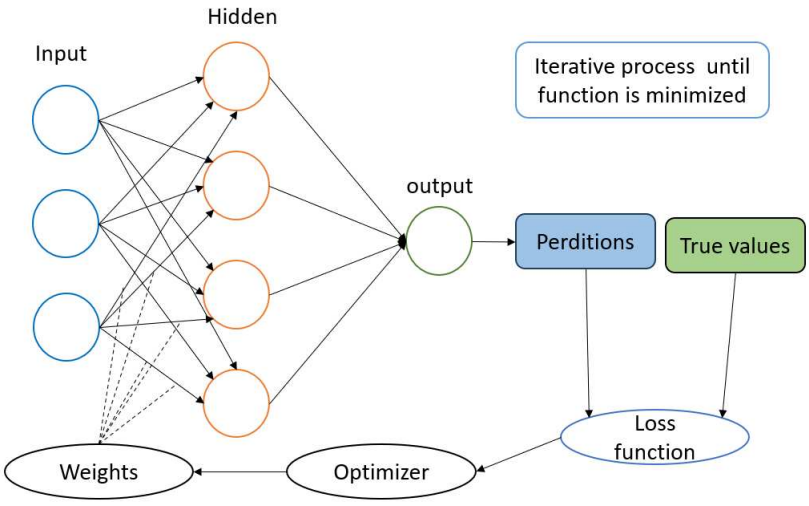

Source: Author.

Each connection between nodes in different layers has a weight associated with it. The model learns the optimal weights during the training process. A bias term is often added to each node to allow for flexibility in the model. Using this methodology the information on the neural network is saved weights and bias, this allows the input-output relation similar to an equation [29].

Originally, neural networks consisted of just input and output layers, forming what is known as a single-layer neural network as shown at Figure 16. However, this configuration

has limitations in evaluating and learning from data due to its low number of layers. For more complex classification rules, it becomes necessary to increase the number of layers [29].

Between the input and output layers, hidden layers are introduced, with each node in a hidden layer performing a weighted sum of its inputs and passing the result through an activation function. This activation function introduces non-linearity into the model, enabling it to learn intricate patterns. Without activation functions, a neural network would simply perform linear transformations, limiting its ability to solve complex problems.

Each node in a hidden layer applies a weighted sum of its inputs and passes the result through an activation function. The activation function introduces non-linearity into the model, allowing it to learn complex patterns.

The activation function determines the output of a node based on its input. Common activation functions include sigmoid, hyperbolic tangent, and rectified linear unit.

Different activation functions can lead to enhanced performances in training, generalization, or computational costs in Neural networks, Laudani et al. [33]. The final hidden layer produces the network's output. The choice of activation function in the output layer depends on the nature of the task (e.g., sigmoid for binary classification, softmax for multi-class classification). An example of the sigmoid function is given by Equation (12).

$$\sigma(x) = \frac{1}{1 + e^{-x}} \tag{12}$$

During the training phase, the neural network learns from a labeled dataset. The model adjusts its weights and biases based on the error between its predictions and the actual labels. To make predictions on new data, the input is fed forward through the network using the learned weights. The output layer produces the final predictions.

2.5.3 Genetic Algorithms

Genetic algorithms, through their ability to explore diverse solution spaces and perform parallel evaluations, provide an advantageous means to address the challenges posed by the multi-variable optimization problem. The iterative nature of genetic algorithms, involving selection, crossover, and mutation, allows for the continuous refinement of the parameter values over successive generations. This iterative refinement enables the algorithm to converge towards an optimal set of stiffness and inertial values that enhance the vehicle's dynamic performance.

GA are optimization algorithms inspired by the process of natural selection and genetics. They belong to the broader class of evolutionary algorithms, which are optimization and search heuristics based on the principles of biological evolution. Introduced by John Holland in the 1960s, genetic algorithms have found applications in various fields, including optimization, machine learning, and artificial intelligence. In order to run GA the understanding of some key components and steps are necessary.

- Initialization: A population of potential solutions (individuals or chromosomes) is generated randomly. Each individual represents a candidate solution to the optimization problem.
- Selection: Individuals are selected from the population based on their fitness, which is a measure of how well they satisfy the optimization objective. Higher-fitness individuals have a higher chance of being selected.
- Crossover (Recombination): Pairs of selected individuals (parents) undergo crossover, where parts of their genetic information are exchanged to create new offspring. This mimics the recombination of genetic material in biological reproduction.
- Mutation: Random changes are introduced into the genetic information of some individuals to simulate genetic mutations. This adds diversity to the population and prevents premature convergence to a sub optimal solution.
- Evaluation: The fitness of the newly created individuals (offspring) is evaluated based on the optimization objective.
- Replacement: The new generation of individuals (offspring) replaces the old generation. This is typically done to maintain a constant population size.
- Termination: The algorithm repeats the selection, crossover, mutation, and evaluation steps for a predefined number of generations or until a termination criterion is met (e.g., reaching a satisfactory solution).

The genetic algorithm iteratively refines the population over multiple generations, with the hope that the population converges toward an optimal solution. This fashion enhances crucial characteristics such as Population-Based Approach. Where population of potential solutions, allowing for exploration of a diverse solution space, as well as, Multiple potential solutions are processed simultaneously, fostering parallelism and increasing the chances of finding a global optimum.

Also GA are effective for global optimization problems, where the goal is to find the best solution in a large and complex solution space. A workflow with the iterative processed is presented in Figure 17.

Genetic algorithms have been successfully applied to various optimization problems, including scheduling, resource allocation, parameter tuning, and feature selection in machine learning. While GA are powerful, their performance depends on appropriate parameter tuning and problem-specific considerations.

In the world of the evolutionary algorithms, the individuals subjected to evolution are the solutions, more or less efficient, for a given problem. These solutions belong to the search space of the optimization problem. The set of the individuals treated simultaneously by the evolutionary algorithm constitutes a population. It evolves during a succession

Figure 17 – GA Workflow

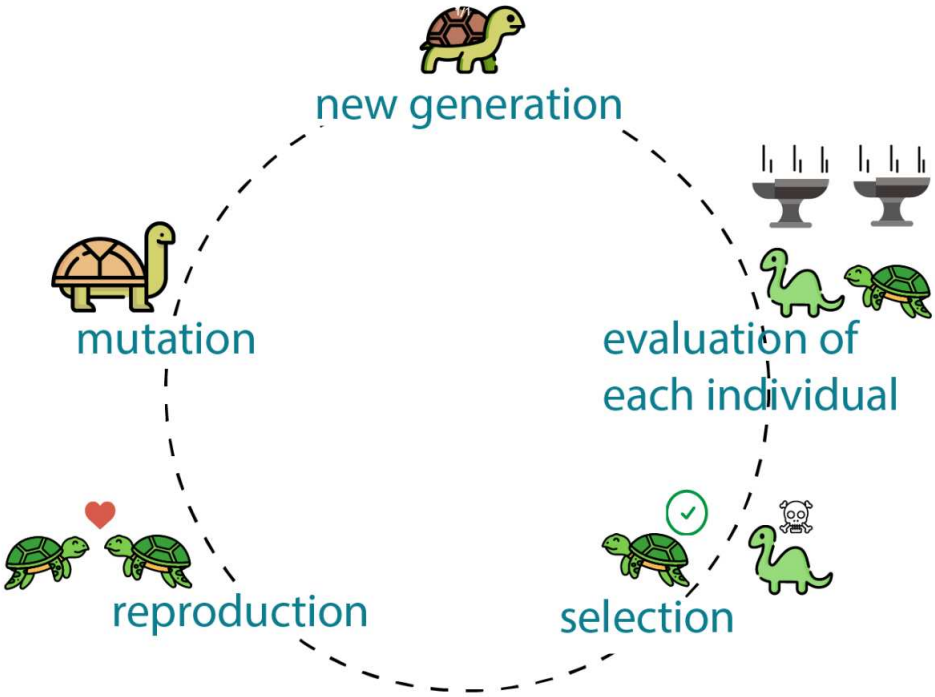

Source: Kumar [32]

of iterations called generations until a termination criterion, which takes into account a priory the quality of the solutions obtained, is satisfied [11].

Also known as evaluation function, the fitness function associates one or multiple fitness (depending if the problem is single or multi objective) values to each individual in order to determine the number of times it will be selected, be it for reproduction or for replacement. The quality of such function can greatly improve the efficiency of a genetic algorithm [11].

From one generation to another, the population is clustered in two distinct groups: the reproduction group and the replacement group. One is not necessarily the complement of the other. The reproduction group contains the individuals that will be reproduced using the crossover and mutation techniques.[11]

3 METHODOLOGY

For an overview of the methodology, the Figure 18 is presented. This flowchart outlines the key steps of the development phases of the master thesis. Starting with Model Parameter Identification, that involves estimating and measuring the parameters necessary for evaluating the implemented model. Then, specific maneuvers are chosen to study parameters under particular vehicle behaviors. After that, The performance of the reference model is compared with the optimized version of the implemented model. This process continues until the termination criteria for each one of the optimized parameter are met.

Figure 18 – Methodology flowchart

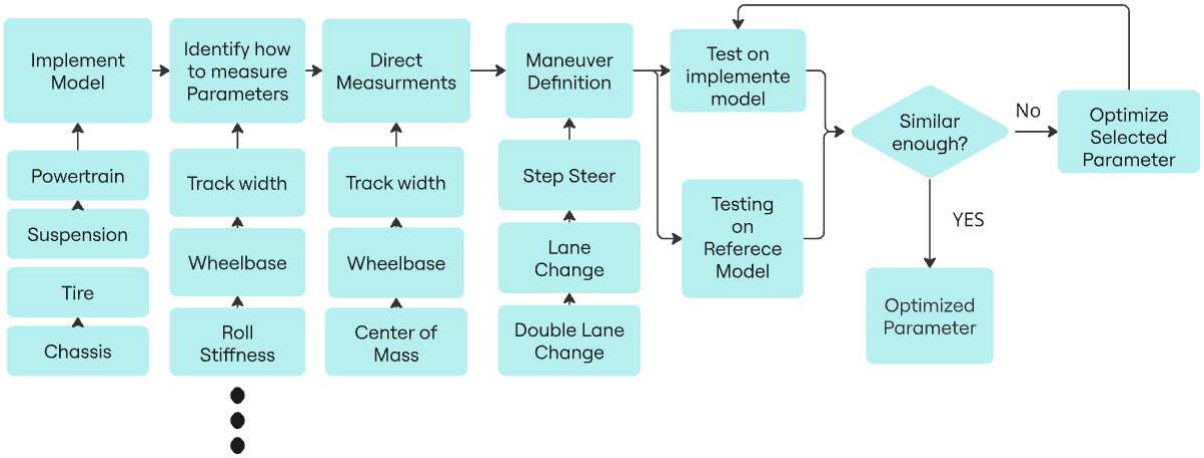

Source: Author.

3.1 IMPLEMENTED MODEL

To estimate the vehicle parameter mathematically is necessary to use a representative vehicle model that considers aspects are evaluated. For that purpose a vehicle twin track model routine was implemented using python language. The vehicle model implemented is characterized by a double track with 10 DoF vehicle model used to study the vehicle behavior in longitudinal, lateral and vertical directions as well as the rotational in each of this directions added to the rotation velocity of each wheel.

Wheel suspension are simply connected to the vehicle chassis by the spring and damper forces, which are applied forces. The chassis is considered to be one rigid body with a full 6 degrees of freedom. Additionally, it shall be assumed that the wheel can only move relative to the chassis in a vertical direction, perpendicular to the road, not being capable represent camber influence in the suspension kinematics.

However is sufficient for initial principle investigations or even for a basic vehicle simulator model [44]. To describe the spatial motion of the chassis, Oe defines a global coordinate system (inertial system) and the motion direction as shown in Figure 19, where Ov is the vehicle coordinate systems.

Figure 19 – Degrees of freedom (DoF) of a spatial twin track model without suspension kinematics.

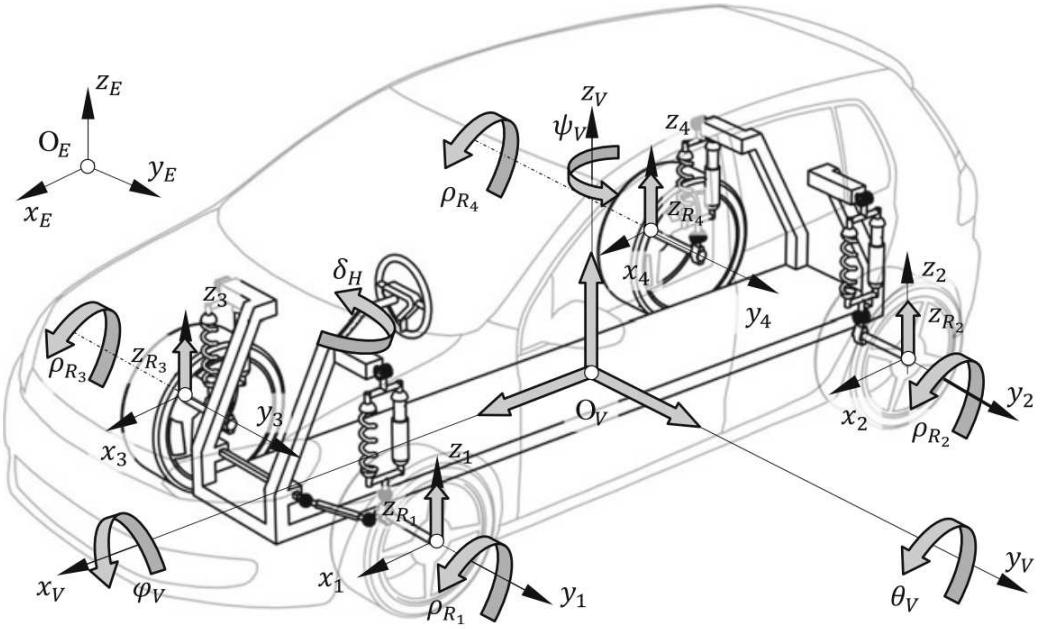

Source: [44]

3.1.1 Model Assumptions and Constrains

To achieve a good balance between complexity and reliability of the model, some assumptions were made. Starting with with the non representation of the unsprung masses and displacements. With that the information about camber change and pneumatic trail were lost.

Also the input range define as throttle position [0, 1], brake position [0, 1], steering position [-1, 1], selected gear $[0, 1, 2, 3, 4, 5, 6, 7, 8]$. The initial condition are represented by the vector:

- Vehicle position and velocity: $x_A = [x, y, z, \phi, \theta, \psi \mid v_x, v_y, v_z\ \omega_x\ \omega_y, \omega_z]$
- Wheel position and angular velocity: $x_R = [\rho_1, \rho_2, \rho_3, \rho_4 | \dot{\rho_1}, \dot{\rho_2}, \dot{\rho_3}, \dot{\rho_4}]$

Figure 20 – Vehicle modules fluxogram

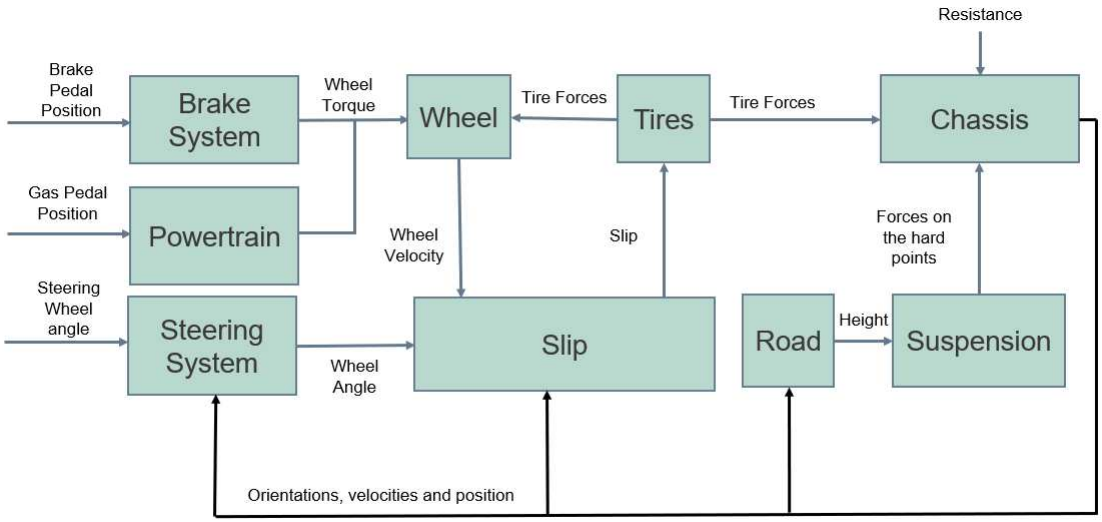

Source: Author.

Some preliminary test and measurement were carried out to determine car static parameter and set a initial state. Starting with determination of CG as described in subsection 3.2.1.

Once the initial condition is defined was possible to calculate initial loads and displacements. To estimate dynamic forces the slip angle used are the presented at subsection 2.1.1 with Pacejka tire model.

The steer angle is assumed the same for both steering wheel, without Ackermann geometry. Camber, caster, toe and other kinematic parameter are not considered in this model, this can lead to some further consideration results. Aerodynamic resistance are considered only on the longitudinal direction (drag coefficient), once the maneuvers made were carried out out in moderate speeds.

This model is composed by modules to describe different systems of the car, each one is responsible for describe one part of the vehicle dynamic. To evaluate the model implemented were carried out test on IPG CarMarker software.

3.1.2 Powertrain model

To elucidate the vehicle's longitudinal performance, it is essential to model several key components. These include the engine's torque and power attributes, the speed and torque ratio of the clutch or torque converter, as well as the gear ratios within the transmission system. With that, the main goal of the powertrain system is to describe the torque applied to the wheels over time and/or as a function of throttle position and engine rpm.

As mentioned earlier, the powertrain plays a crucial role in supplying torque to the vehicle wheels. Regarding the powertrain model implemented, the essential inputs include

the following parameters:

- throttle: a value between 0 and 1, indicating the position of the throttle.
- brake pedal: a value between 0 and 1, indicating the position of the brake pedal.
- $torque_{max}$ table: a vector containing the maximum torque values corresponding to the RPM values in *rpm* table, as follows in Figure 21.

Figure 21 – Engine torque x Engine RPM

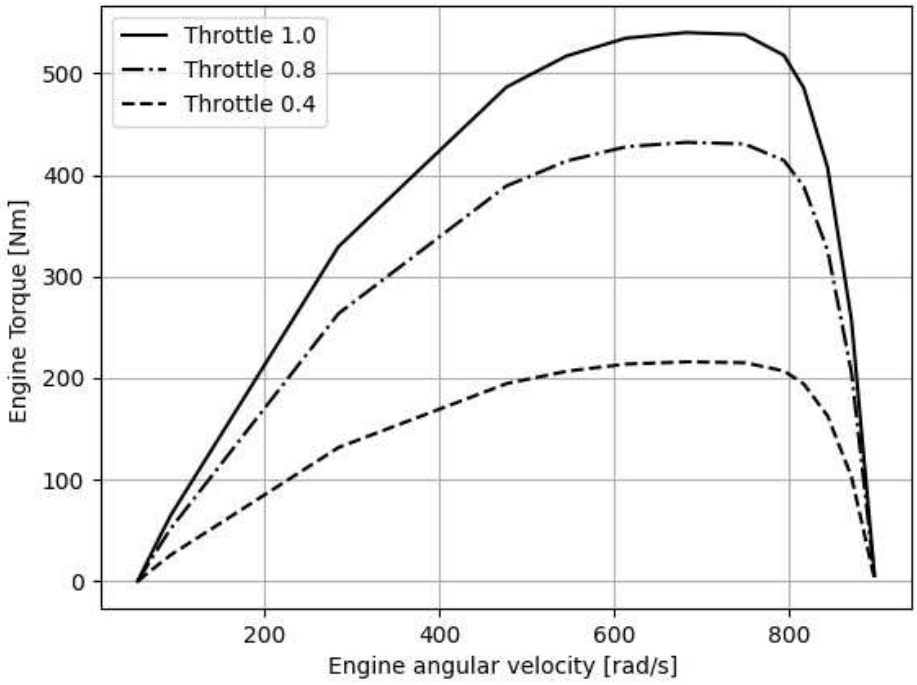

Source: Author

The method first uses interpolation function to access the maximum torque available at the engine for the current engine RPM value. The available torque will be further multiplied by the throttle position to access the net torque provided by the engine. A specific engine case is shown in Figure 21 to demonstrate how the torque available can be calculated.

To establish the final speed ratio between the engine and the vehicle's wheels, it is essential to select the appropriate gear and determine the torque converter speed ratio. This is done by utilizing the vehicle speed in the last time step and comparing with the engine rotation at the current time step. Where the current engine rpm takes the previous engine rpm, and check with the gear was changed.

When the gear is changed the new value of rpm is defined by the torque applied at the last time stamp and the inertial of the engine.

Gear selection is based on a table that correlates engine speed rotation with throttle position, specifically tailored to each engine aiming for the best efficiency and performance, as shown in Figure 21. This table establishes the upper limits that trigger shifting of gears. Notably, when the vehicle decelerates, downshifting occurs with respect either to a lower limit in RPM given a certain throttle position, or as depicted by the Table 5.

Table 5 – Car Maker Gear Selection

Gear	**Throttle**	**Min RPM**	**Max RPM**
1	0.0	1000	2750
1	0.4	1000	2750
1	0.8	1000	5250
1	1.0	1000	2500
2	0.0	1000	2500
2	0.4	1000	2500
2	0.8	2000	5000
2	1.0	2000	5000
3	0.0	1250	2500
3	0.4	1250	2500
3	0.8	2250	5000
3	1.0	2250	5000
4	0.0	1500	2000
4	0.4	1500	2000
4	0.8	2500	4500
4	1.0	2500	4500
5	0.0	1750	6000
5	0.4	1750	6000
5	0.8	3000	6000
5	1.0	3000	6000

Source: Author.

Gear ratio is defined according to the criteria mentioned in the appendix and it is depending on the particular vehicle. With the intention of representing the powertrain interactions with the vehicle dynamics a powertrain class is responsible for calculating the current engine torque transmitted to the wheels. According to [44], the final output torque in each wheel can be calculate in the front and rear axle respectively by the Equation (13). The Brake system is integrated into the powertrain once the parameters of interest for further calculation is the wheel torque net.

For the sake of simplicity, the equation below illustrates a scenario where all four wheels receive the same torque as follow in Equation (13). This can be fine-tuned by introducing a bias for front/back differential transmission in cases where it better represents the vehicle dynamics.

$$M_{R_1,a} = M_{R_3,a} = \frac{1}{2} i_v i_D [i_G M_k - \frac{1}{i_G} [\theta_{GI} i_G^2 + \theta_{GA}] \alpha_m] \tag{13}$$

Where:

- $i_G(G)$ - gear ratio (gear-dependent),
- i_D - gear transmission ratio of the central differential,
- θ_{GI} moment of inertia of the engine-sided driveshaft,
- θ_{GA} moment of inertia of the drivetrain-sided driveshaft

Once the engine net torque $engine_{torque}$ is accessed part of this torque is used to update the engine speed $engine_w$ for the next time step. This is done by calculating the angular acceleration of the engine $engine_{wdot}$ as in Equation (14) and then integration on each time step:

$$engine_{wdot} = (engine_{torque})/engine_{inertia} \tag{14}$$

After that the engine angular speed is calculate by integrating the Equation (14) as follow in Equation (15).

$$engine_w = (engine_w + engine_{wdot} * time_{step}) \tag{15}$$

In the context of automatic transmissions, the torque converter plays a crucial role in modulating both torque and speed transmitted to the transmission. This modulation relies on the input and output rotation ratios, the torque gain provided can be calculated by Equation (16). The torque converter ratio ranges from 2.3 to 1.0, contingent on the speed ratio. Specifically, at a speed ratio close to 0, the torque ratio is 2.3, and at a speed ratio of 1, the torque ratio shifts to 1.0 when the clutch is engaged.

$$Speed_{ratio} = rpm_{turbine}/rpm_{pump} \tag{16}$$

Alternatively, one can use a manual transmission system, which simplifies the process to either being with the clutch engaged or disengaged. Consequently, torque and engine rotational speed are directly transmitted, and a blending function is employed to soften the abrupt changes that can occur during gear shifts. The ultimate output of the powertrain reveals itself as the final transmission ratio. This ratio is contingent upon the interplay of gear ratios, torque converter ratios, and differential ratios. Mathematically expressing Equation (17).

$$final\ ratio = i_g i_c i_d \tag{17}$$

Where:

- i_g: gear ratio
- i_c: converter torque or clutch speed ratio
- i_d: differential ratio

3.1.3 Wheel and tire model

The wheel system is divided into modules responsible for computing the wheel angular velocity, longitudinal slip or $slip_x$ and lateral slip α for each wheel, followed by the forces of iteration with the ground.

3.1.3.1 Slip calculation

To accurately compute the forces arising from tire interaction, it is essential to assess tire slip in both the longitudinal and lateral directions. To achieve this, the required inputs include the wheel dynamics radius r_{dyn}, the vehicle's longitudinal speed v_x, lateral speeds v_y, and also the wheel angular velocity $wheel_{wvel}$. Equation (18) and Equation (19) describe the slip calculation in the longitudinal and lateral directions respectively:

$$slip_x = \frac{(r_{dyn} wheel_{wvel}) - v_x}{max(|r_{dyn} wheel_{wvel}|, |v_x|)} \tag{18}$$

$$\alpha = -arctan\left(\frac{v_y}{max(|r_{dyn} wheel_{wvel}|, |v_x|)}\right) \tag{19}$$

Constraints were incorporated into the implementation to ensure that v_x and $wheel_w$ are either positive or zero. This ensures that the vehicle is either moving forward or stationary. The wheel angular speed is obtained by integrating the ground interaction force over the last time step, and this process is reiterated at each time step. Meanwhile, the x_y is derived from the chassis modules, employing a similar logic based on the integration of the vehicle body acceleration in accordance with Newton's Second Law.

3.1.3.2 Tire model applied

The tire module in the implementation employs the empirical Magic Formula Tire Model, introduced by Prof. Hans Pacejka in 1987. This formula utilizes the pure slip condition to determine one of three parameters by substituting the inputs: The longitudinal force F_x as a function of longitudinal $slip_x$. The lateral force F_y as a function of $slip_y$. The aligning moment Mz as a function of $slip_x$. The mathematical description of is shown at Equation (20) and Equation (21).

$$y(x) = Dsin[CarctanBx - E(Bx - arctan(Bx))] \tag{20}$$

Considering that Y is the desired output, with the input X, being $slip_x$ or $slip_y$.

$$Y(X) = y(x) + S_v \tag{21}$$

with:

$$x = X + S_h \tag{22}$$

Here, the parameters are empirically estimated, or for the sake of simplification, literature values can be applied:

- B: stiffness factor
- C: shape factor
- D: peak factor
- E: curvature factor
- S_h: horizontal shift
- S_v: vertical shift

This approach allows for the calculation of contact forces in each of the four wheels in both the longitudinal and lateral directions.

3.1.4 Steering System

The function yields a steering wheel angle, which is subsequently utilized to compute the lateral forces at the tire modules. These modules transform the steering input, ranging from -1 to 1, into wheel steering δ, and calculate the steering speed to stay within an anthropomorphically plausible range. The displacement of the steering wheel is also constrained and adhered to the vehicle‘s specifications. Further details regarding the mathematical description can be found in the attached code.

3.1.5 Chassis and suspension model

The chassis is computed using the Newton law of motion and is segmented into two modules. The initial module computes translation motion, while the latter manage the rotational movements. The suspension is modeled as a torsional spring and damper system acting around the roll axis, illustrated in Figure 22. Pitch and yaw moments are calculate similarly.

To derivate the translation equations is assumed that non-inertial frame S_v is translating with velocity v relative to the a O_E, as showed at Figure 19. Due to the center mass of the vehicle is attach with the origin of O_v, the equations are derived with the vehicle frame O_v.

The translation integrals are represented by the Equation (23),Equation (24) and Equation (25) in the x, y and z directions respectively. Where the output value is updated each time step.

Figure 22 – vehicle roll model.

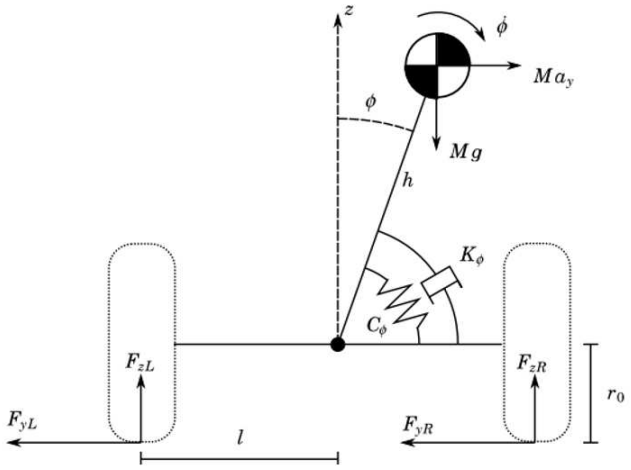

Source: Castro, Rill, and Weber [8]

$$acc_x = \frac{F_x}{m} + v_y\dot{\psi} + h[sin(\theta)cos(\dot{\phi})(\dot{\psi}^2 + \dot{\theta}^2 + \dot{\phi}^2) - sin(\phi)\ddot{\psi} - 2cos(\phi)\dot{\phi}\dot{\psi} - cos(\theta)cos(\phi)\ddot{\theta} + 2cos(\theta)sin(\phi)\dot{\theta}\dot{\phi} + sin(\theta)sin(\phi)\ddot{\phi}] \tag{23}$$

$$acc_y = F_y/m - vx\dot{\psi} + h(-sin(\theta)cos(\phi)\dot{\psi}dot - sin(\phi)\dot{\psi}^2 - 2cos(\theta)cos(\phi)\dot{\theta}\dot{\psi} + sin(\theta)sin(\phi)\dot{\phi}\dot{\psi} - sin(\phi)\dot{\phi}^2 + cos(\phi)\ddot{\phi}) \tag{24}$$

$$acc_z = ((F_z - mg)/m) \tag{25}$$

According to Castro, Rill, and Weber [8] the rotational movements can be assessed by the following equations:

$$\ddot{\phi} = [h(F_yTcos(\phi)cos(\theta) + mgsin(\phi)) - C_\phi\phi - K_\phi\dot{\phi} + \dot{\psi}(I_y - I_z)(\dot{\psi}sin(\phi)cos(\phi)cos(\theta) + \dot{\phi}sin(\theta)sin(\phi)cos(\phi)) + \dot{\psi}\dot{\phi}(I_ycos^2(\phi) + I_zsin^2(\phi))]/ [Ixcos^2(\theta) + I_ysin^2(\theta)sin^2(\phi) + I_zsin^2(\theta)cos^2(\phi)] \tag{26}$$

$$\ddot{\theta} = [h(mgsin(\theta)cos(\phi) - F_xcos(\theta)cos(\phi)) - C_\theta\theta - K_\theta\dot{\theta} + \dot{\psi}(\dot{\psi}sin(\theta)cos(\theta) (I_x - I_y + cos^2(\phi)(I_y - I_z)) - \dot{\phi}cos^2(\theta)I_x + sin^2(\phi)sin^2(\theta)I_y + sin^2(\theta)cos^2(\phi)I_z) - \dot{\theta}(sin(\theta)sin(\phi)cos(\phi)(I_y - I_z))]/[I_ycos^2(\phi) + I_zsin^2(\phi)] \tag{27}$$

$$\ddot{\psi} = [M_z T - h(F_x sin(\phi) + FyTsin(\theta)cos(\phi))][Ixsin^2(\theta) + cos^2(\theta)(I_y sin^2(\phi) + I_z cos^2(\phi))] \tag{28}$$

F_x, F_y, and F_z denote all the forces in the x, y, and z directions, respectively, acting on the vehicle's center of gravity (CG). Meanwhile, C_θ and K_θ represent the equivalent inertias in pitch and roll moments. All the equations implemented are available in the appendix

3.2 DATA COLLECTION

In order to validate the implemented model, collection of virtual and real data test are required.

3.2.1 Center of mass

The vertical loads of tires transferred during maneuvers that involve acceleration, whether vertical or longitudinal, are strongly influenced by CG. To experimentally measure these parameter with a static test, an alternative is to use the load transfer induced in the inclination of a vehicle axis. First, the vehicle is placed on a flat surface measure the mass on each wheel. Doing this procedure is possible to estimate the x coordinate of CG using wheelbase and the y coordinate with track width, as showed in Equation (29) and Equation (30) respectively.

$$\begin{aligned} \sum M_Y &= 0 \\ 0 &= -W_{front} X_{CG} + W_{rear}(X_{Wheelbase} - X_{CG}) \\ X_{CG} &= \frac{W_{rear} X_{Wheelbase}}{Wfront + W_{rear}} \end{aligned} \tag{29}$$

$$\begin{aligned} \sum M_X &= 0 \\ 0 &= -W_{left} Y_{CG} + W_{right}(Y_{tranckwidth} - Y_{CG}) \\ Y_{CG} &= \frac{W_{right} Y_{trackwidth}}{W_{left} + W_{right}} \end{aligned} \tag{30}$$

Then to find out the center of gravity height, the front axle is elevated with parallel fix to the ground. An angle near $\theta = 45$ degrees is preferable to minimize errors due to trigonometric functions. Knowing the vehicle wheelbase and height that front axle was raised above the ground and the new allow to the θ angle with Equation (31).

$$\theta = sin^{-}1\left(\frac{DE}{Wheelbase}\right) \tag{31}$$

Figure 23 – Center of Gravity Height.

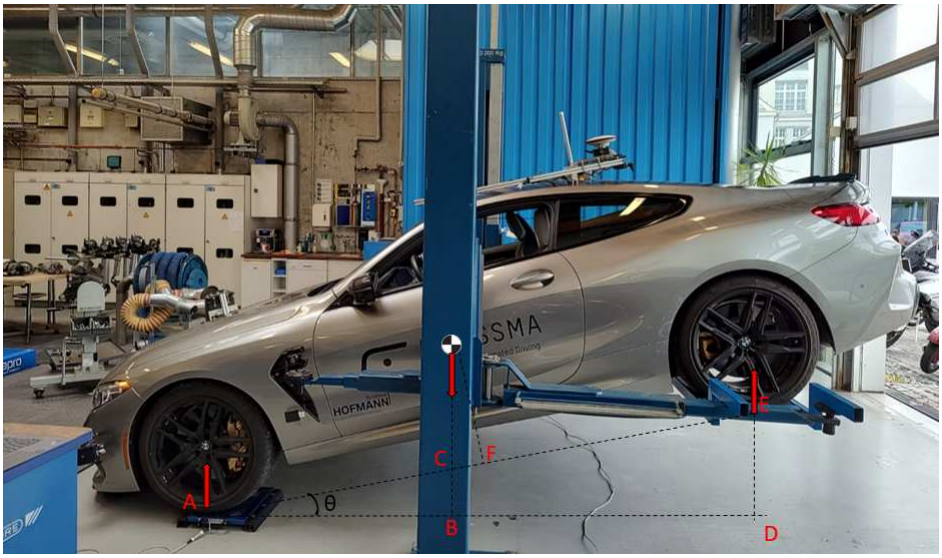

Source: Author

Thus, the CG height is calculate using Equation (32) where W_{total} is the vehicle mass at the center of mass. The distance are shown in Figure 23.

$$\begin{aligned} \sum M_Z &= 0 \\ 0 &= W_{total}AB - W_{rear}AD \\ AB &= \frac{W_{rear}AD}{W_{total}} \\ AC &= \frac{AB}{cos\theta} \end{aligned} \tag{32}$$

Thus using trigonometric relationship, we find Equation (33).

$$\begin{aligned} CF &= AE - AC - X_{cm} \\ CG_{height} &= \frac{CF}{\tan\theta} \end{aligned} \tag{33}$$

It was assumed that the displacements of the front and rear suspensions are equal, as well as deformation of the tire has no influence on the load. To mitigate error an usual approach of measuring in different angles and than apply the mean. It has to be point out the any addition of equipment, fuel or passenger will affected this parameter.

3.2.2 Vehicle

The primary vehicle utilized in this study is a BMW M8 Competition equipped with an all-wheel-drive (AWD) layout. Vehicle parameter measurements were conducted at THI facilities, augmented with additional equipment including measurement systems, GPS, and IMU.

The IMU unit was affixed to the roof of the vehicle in a predetermined position. It captured longitudinal, lateral, and vertical accelerations, as well as roll rate, pitch rate, and yaw rate of the chassis. Concurrently, the GPS system recorded the vehicle's location, heading, speed, and acceleration. To ensure accurate data interpretation, coordinate transformations were employed to transfer measured values from the sensor location to the vehicle's center of mass [14].

Figure 24 – Acquisition System and supply battery.

Source: Author

As illustrated in Figure 24 the acquisition system is positioned above the computer, while the IMU unit is strategically placed in the backseat area, as close to the vehicle's center of gravity as possible. It is imperative to note that the addition of these devices introduces weight and alters the vehicle's load distribution, factors that must be accounted for in the vehicle model.

3.2.3 Maneuvers

The first maneuver performed was acceleration-rolling-braking going from 0 m/s to $8m/s$, $18m/s$ and $25m/s$ respectively under the CM and at the Implemented model. Figure 25 show the representation of the test track marked with cones to shown the transitory events of this test.

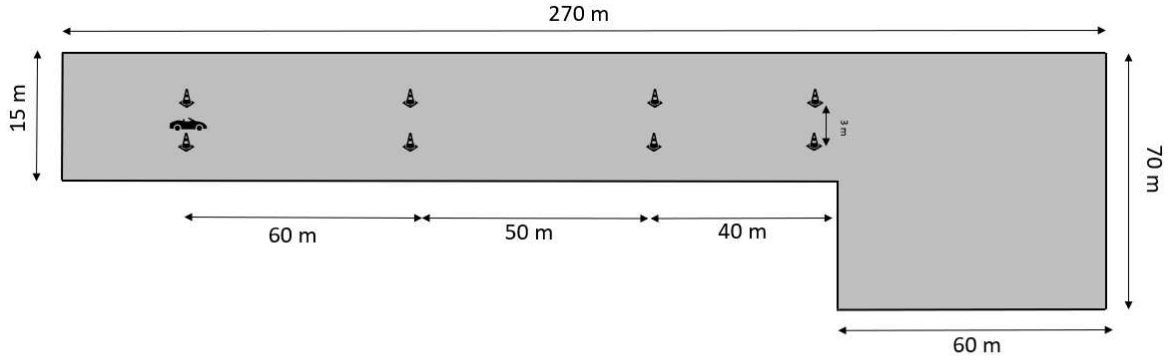

Figure 25 – Acceleration and brake

Double lane-change according with ISO 3888-2 recommendations. The configuration employed in the test track is illustrated in Figure 26. The assessed speeds remained consistent throughout all maneuvers, maintained at 8, 18, and 25 m/s.

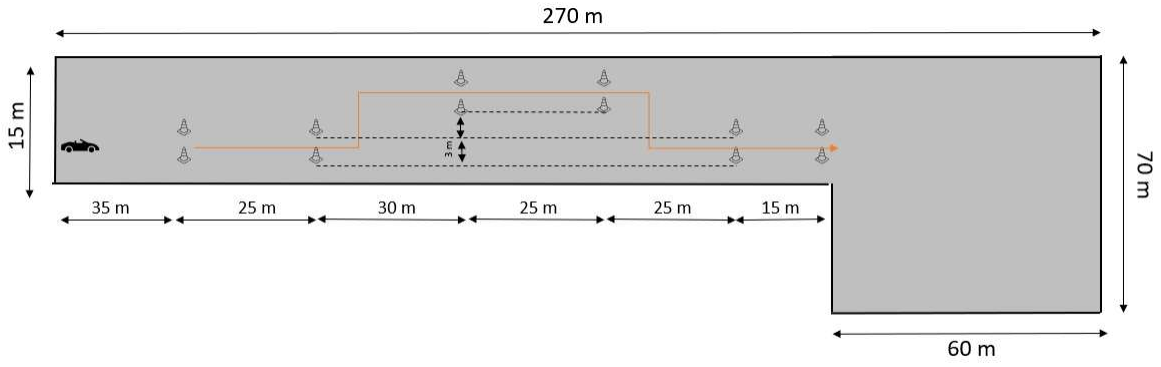

Figure 26 – Double lane change

Steer steps were executed under a constant speed of 8, 13, and 18 m/s in a circular path with an external diameter of 45 meters, as depicted in Figure 27. This was done to assess the steady dynamic behavior under roll and the maximum lateral accelerations.

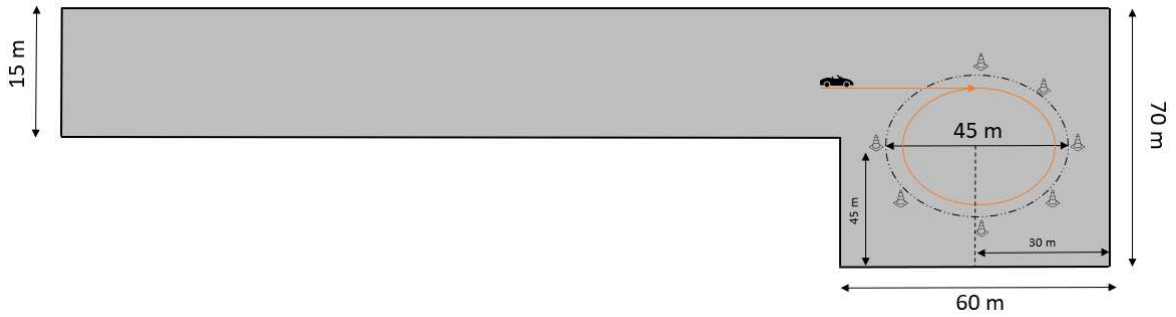

Figure 27 – Step steer

3.2.4 Virtual

The virtual data was collected with the help of CM. The same input parameter are set for the manoeuvres such as double lane change and step steer. The virtual scenario was build according to ISO3888-2:2011.

The validity was determined by the Yaw rate, tire slip angle, lateral accelerating results in step steer test. As well as the double lane change were evaluated roll angle and roll rate trend. Once the implemented model proved to follow same trends is to pursue the following optimizations. This data is used to adjust the model performance by applying the "optimization method".

3.3 OPTIMIZATION

In the current study, the focus revolves around optimizing the inertial and stiffness values within a dynamic system. To address the challenge of contamination, the optimization is conducted in a modular fashion, allowing for a systematic approach to mitigate potential issues. This study applies genetic algorithms GA for optimizing the stiffness and inertial values within a vehicle model. It first, it was carried out the optimization problem with to specific parameters that significantly impact the v_x. Among those parameter it was possible to highlight Gear Box Inertia, Engine Inertia, Wheel Inertia, Drive Shaft Inertia. Table 6 at 4.5 shows the ranges within these parameters were evaluated.

4 RESULTS

In this section the results from the implemented model and the CM will be compared in terms of dynamic response using the same inputs. Additionally, this study will present some of the vehicle test results alongside the outcomes derived from the optimized parameters.

4.1 POWERTRAIN BEHAVIOUR

To ensure an accurate representation of vehicle dynamics, it is essential to assess the modules response of initial interaction with external input. In the powertrain module, this assessment involved implementing an acceleration manoeuvre using input data sourced from IPG CarMaker. This procedure enables a through validation of the model's fidelity in terms of longitudinal velocity, gear change behavior, and powertrain net torque.

Figure 28 – Gear selection response.

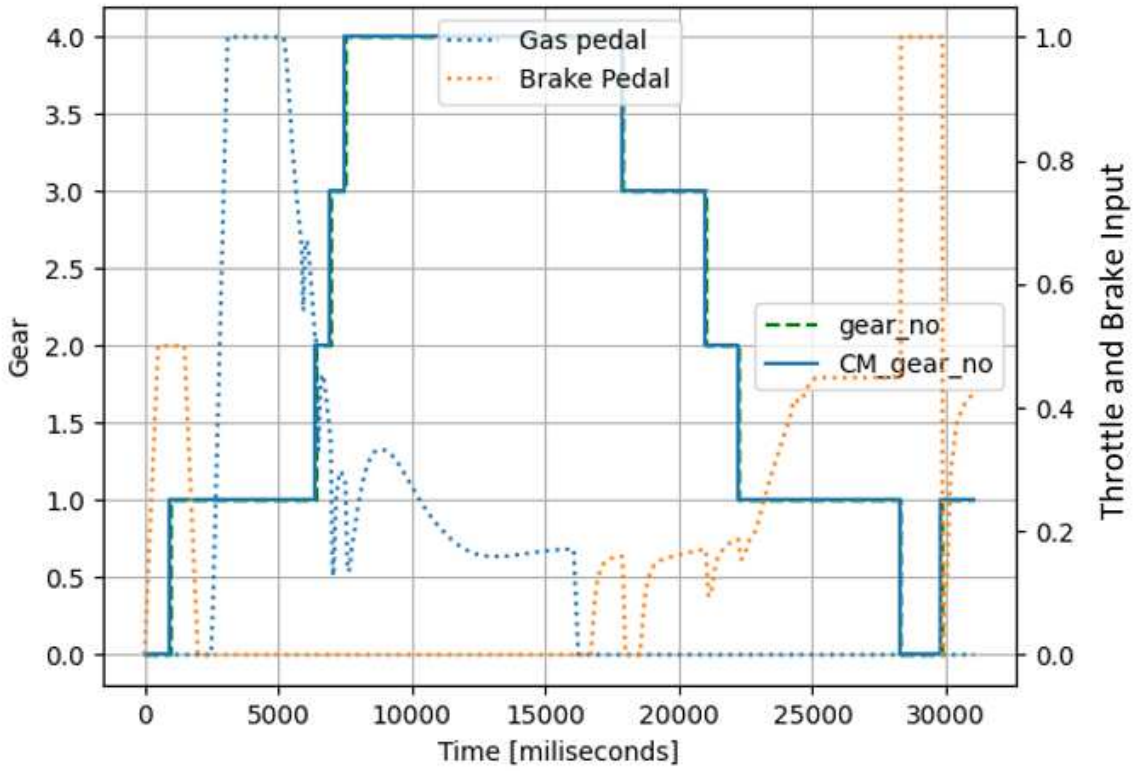

Source: Author

In the Figure 28 is showed the throttle and brake pedal inputs applied in the acceleration and braking manoeuvres in the CMsoftware, the most important outputs to verify in the powertrain module of the code implemented are gear selected and a

correspondent torque at each wheel. To verify the vehicle behaviour the constrains of the IPG model to change gear were reproduced and gear number appear being almost identical, only with one step delay in the implemented model. Accurate approximation becomes feasible thanks to the ability to verify the IPG CM constraint for gear selection.

Meanwhile, the torque can be verified at Figure 29 the vehicle torque provide can be negative, meaning that the vehicle is deceleration either by pedal brake action or be the engine resistances.

Figure 29 – Longitudinal velocity.

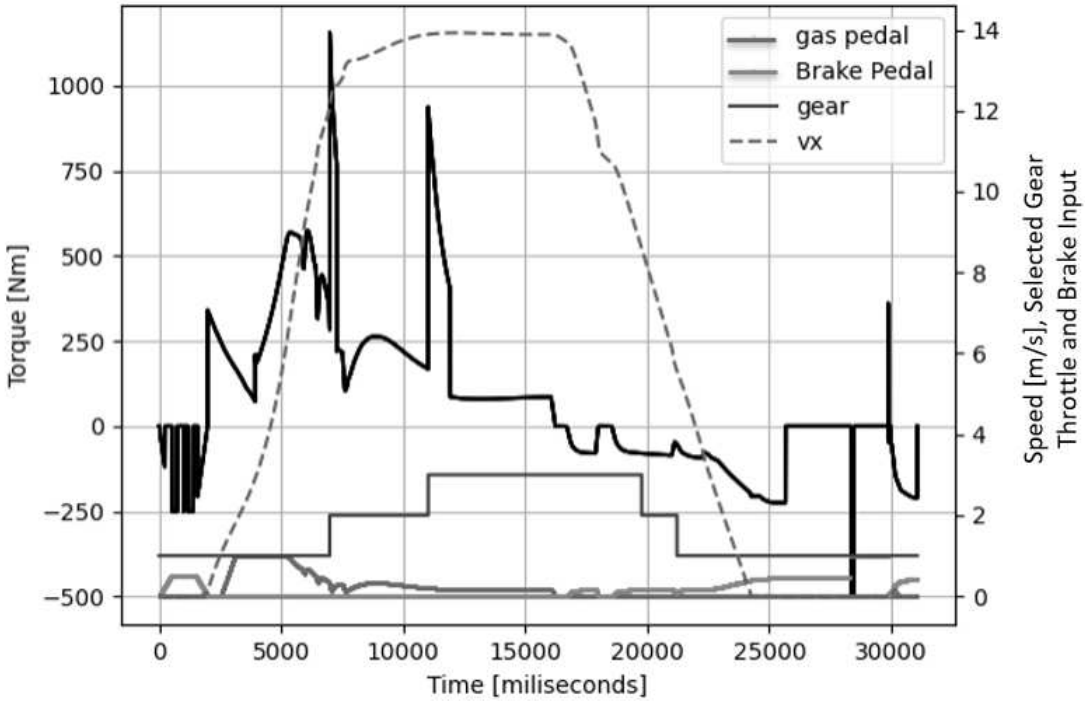

Source: Author

This implies the deliberate implementation choices made to maintain the feasibility of a net torque transfer from throttle and brake inputs to the wheels within the same module.

Therefore, the net torque of the powertrain is depicted in Figure 29, and its characteristics are influenced by the throttle, gear selection, and engine angular speed, ultimately determining the delivered torque. The spikes in the torque can be attributed to gear change processes, during which the torque converter experiences varying input and output speeds.

However, these spikes quickly converge to the transmission ratio when a locked clutch is considered. It is also observed that the engine speed remains stable and does not fluctuate in the same manner as the torque output. Results of the longitudinal velocity v_x in the vehicle achieving 14 m/s within a 11 second time, almost identify results were verify in the IPG CarMaker, being this the ultimate consequence of the powertrain module for the model.

In Figure 30, the engine angular speed is depicted, showcasing its correlation with the vehicle speed and selected gear ratio. Notably, the graph illustrates a smooth trend without the spikes observed in torque output. The gas and brake pedal inputs over time are also visualized in the same Figure 30. In the same image, the black line illustrates the torque, allowing us to observe an increase in wheel torque with throttle input. When the brake is engaged, the torque becomes negative.

Figure 30 – Torque output.

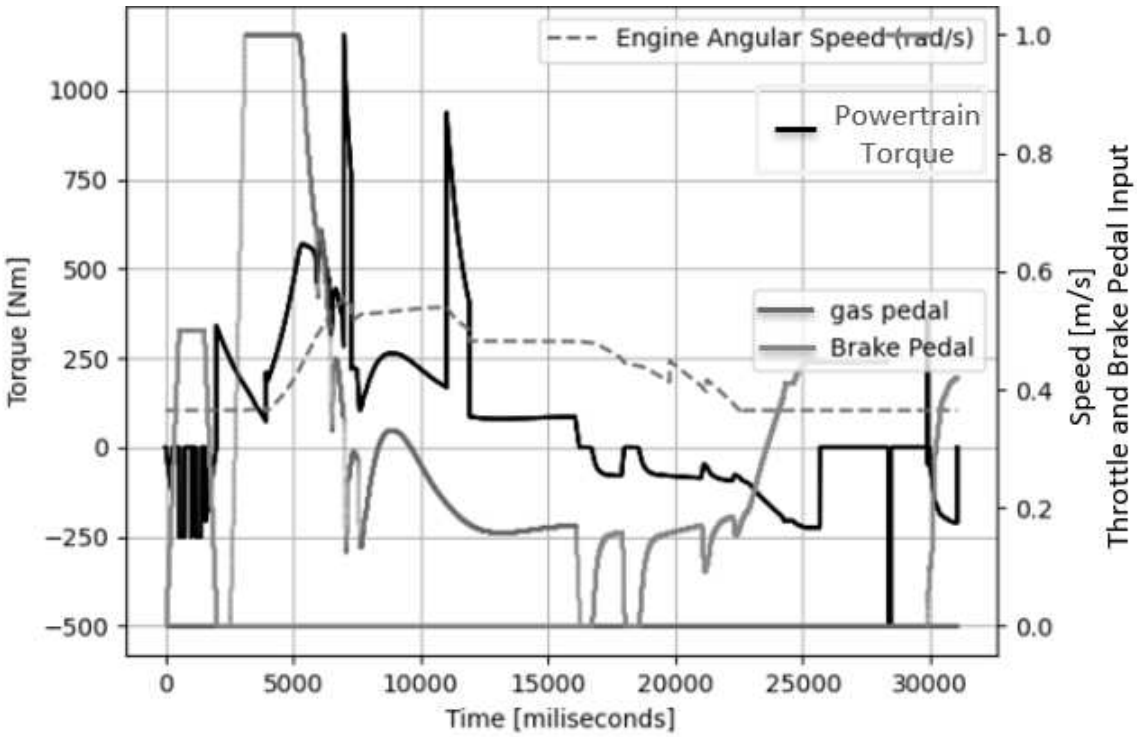

Source: Author

4.2 ROLLING AND BRAKE TEST

Since this test is for longitudinal motion, the most important data to compare is longitudinal acceleration and pitch rate. To evaluate to implemented model the pitch along with throttle and longitudinal acceleration are plotted at Figure 31. At Figure 31 is the correlation between the longitudinal acceleration acc_x and the pitch angle can be , while the gear is kept constant at the 1 st gear. The acceleration, acc_x, remains within the range of -2 and 2 m/s^2, which is a reasonable value for longitudinal motion. Meanwhile, the pitch stays negative during acceleration and shifts to the positive side when the brake is applied.

In the context of Figure 32, it is notable that the pitch rate exhibits similar patterns to those observed in the CM test, with more pronounced spikes in the CM model. These

Figure 31 – Pitch and Longitudinal Acceleration.

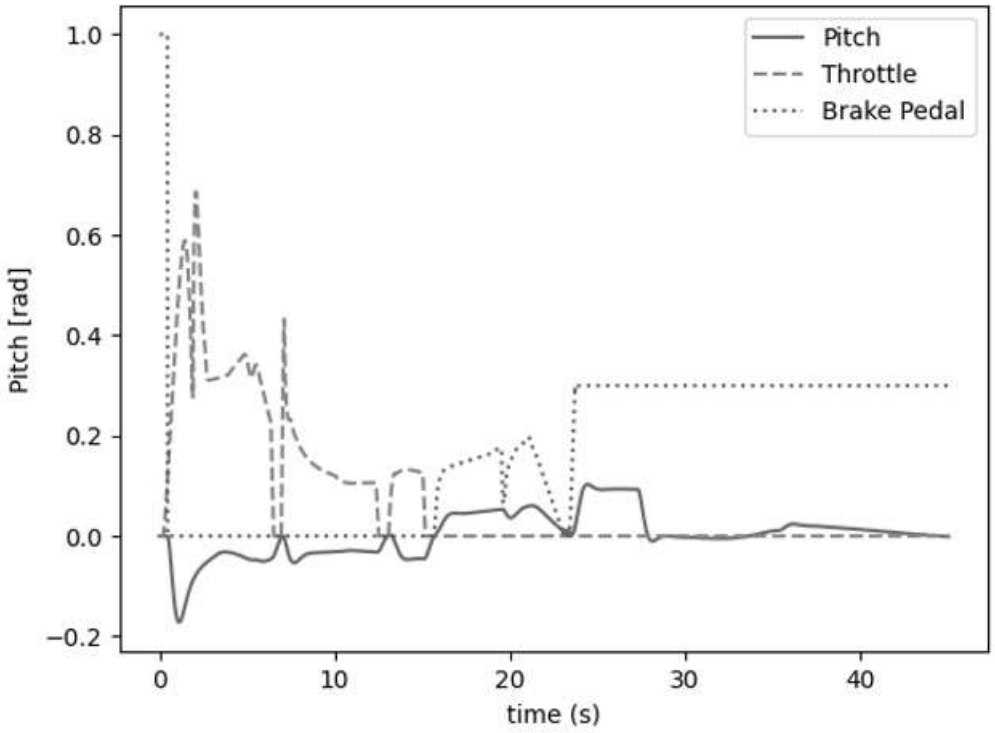

Source: Author

variations in pitch rate are attributed to the release of the throttle during gear shifts. This observation implies a potentially lower resistance input for pitch in the implemented model, and adjustments can be considered during optimization if deemed necessary. Nonetheless, evaluating the pitch rate poses challenges due to its relatively small values, making it difficult to isolate and assess this parameter independently.

Another observation is that the brake and powertrain system model currently in use only takes into account the driving wheels for acceleration and braking. This model overlooks the coupling effects resulting from mechanical and fluid interactions, potentially leading to a less accurate representation of real-world scenarios.

Furthermore, the CM model being compared does not disclose all its equations, adding complexity to understanding the differences from the implemented model. This lack of transparency makes it challenging to identify specific variations between the two models. In general, achieving precise behavior necessitates a complete system that account all relevant factors.

4.3 STEP STEER TEST

The step steer maneuver is commonly employed as a highly effective method for assessing a vehicle's yaw response and lateral acceleration, representing the acceleration

Figure 32 – Pitch Rate at Longitudinal Acceleration.

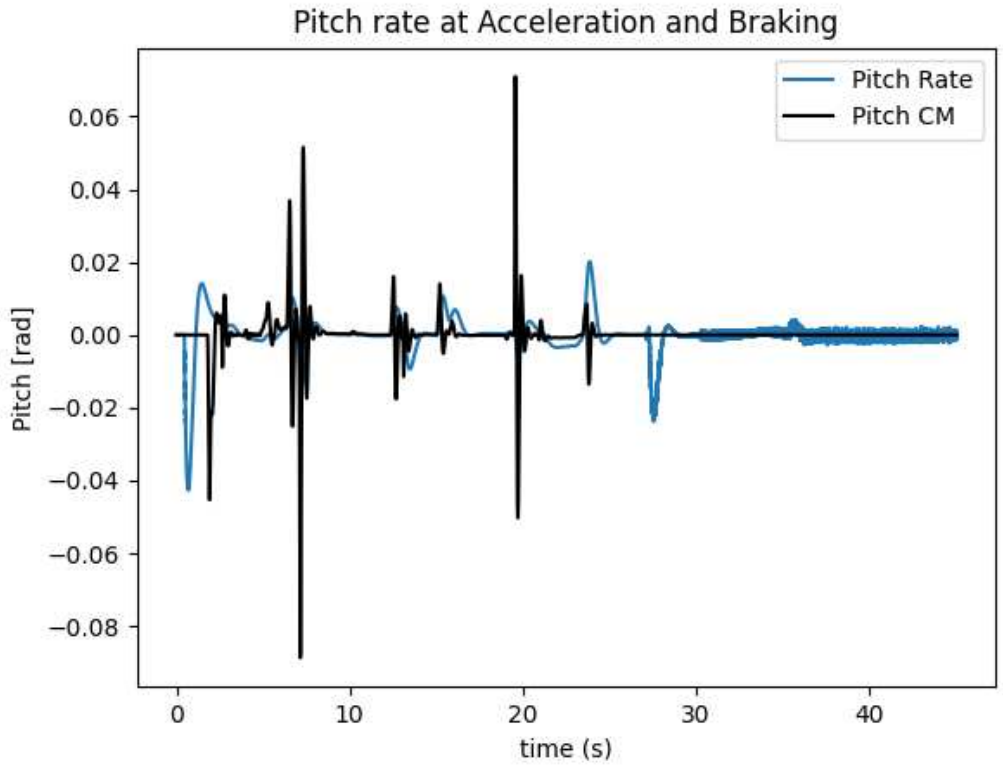

Source: Author

experienced in the sideways direction. Despite its effectiveness, the practicality of conducting a graphical comparison of yaw was hindered by global coordinate adjustments, aimed at preserving the operation of other modules. Although the yaw in the CM model had the potential for infinite extension, the implemented model introduced a constraint. This limitation cut down the steering angle upon completing a full circle, consequently restricting yaw and ensuring a more controlled and manageable simulation environment.

From the model implemented data, is possible to see at Figure 34 that the yaw response is almost immediately after the steering input with a peak lag within 0.3 seconds. Indication a quick response of the vehicle both in yaw and roll responses.

Step steer testing helps can be useful to determine understeer or oversteer tendency of the vehicle. These characteristics are crucial for understanding the vehicle's balance and handling stability. In that sense the slip at each wheel or the wheel forces can be helpful to understand this behavior. Taking the adjust in steering angle mentioned before, Figure 33 presents the forces at each wheel that is depended on the slip and vertical load applied to Tire Magic Formula. The Fy index represents the force that the tire is supporting in the lateral direction, while Fx represents the force in the longitudinal direction. Meanwhile, FL, RL, FR, and RR stand for the front left, rear left, front right, and rear right wheels,

respectively. The graphic indicates the front external wheel presents the greater value while the rear internal the lower one.

Figure 33 – Wheel Forces At Step Steer.

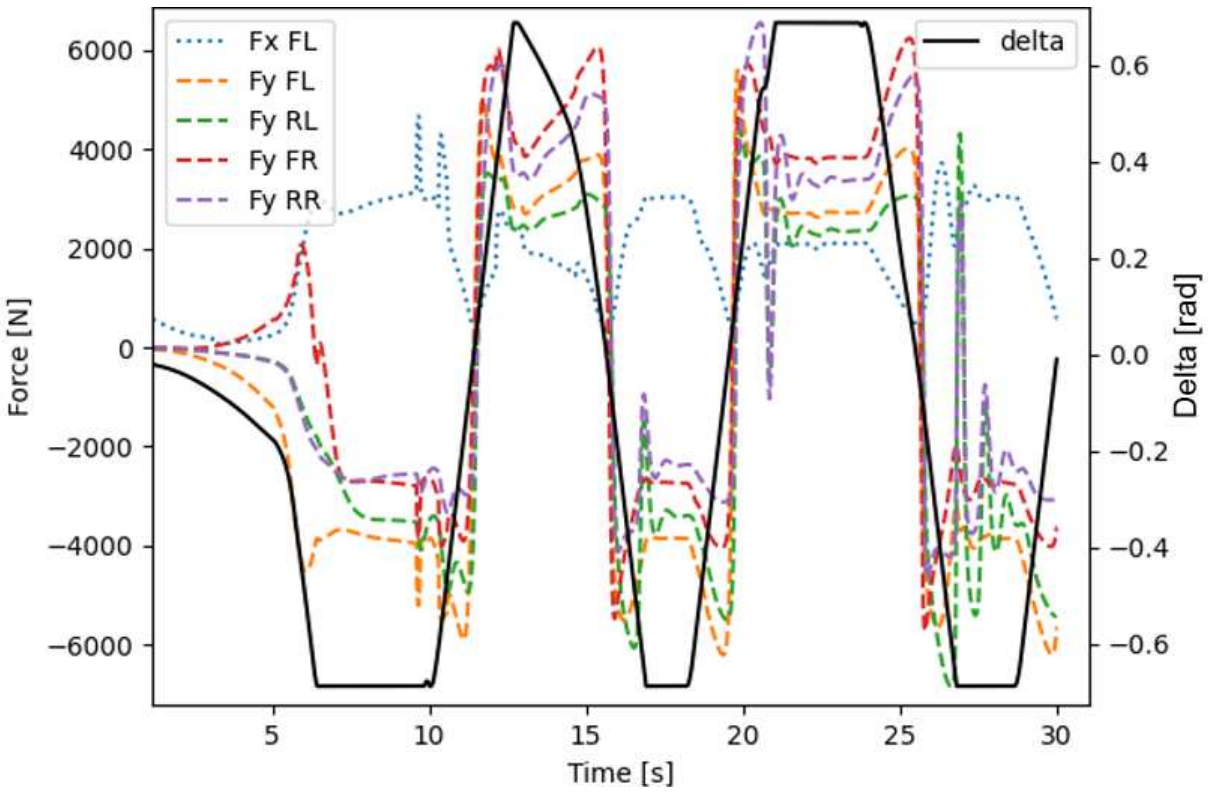

Source: Author

Analyzing the forces at each wheel during a step steer maneuver provides crucial insights into the distribution of lateral loads and tire contributions. The front external wheel, as indicated in Figure 33, exhibits a higher force, suggesting increased lateral grip and load transfer to the outer tire during the turn.

Conversely, the lower force observed at the rear internal wheel implies a relatively reduced lateral load transfer to the inner tire. This can be associated with the tendency for the rear of the vehicle to experience less lateral weight transfer, contributing to overall stability. The interplay between these forces and the corresponding slip angles at each wheel provides a comprehensive understanding of the vehicle's dynamic response to steering inputs.

Moreover, the variation in wheel forces highlights the importance of tire characteristics, such as lateral stiffness and cornering capabilities. The Tire Magic Formula, accounting for slip angle and vertical load, proves instrumental in modeling these forces accurately. By linking the steering input adjustments to the resulting forces at each wheel, engineers gain a deeper understanding of the intricate relationship between tire behavior, lateral load transfer, and the vehicle's stability profile.

4.4 LANE CHANGE

Lane change vehicle dynamic testing is designed to assess a vehicle's behavior and performance during rapid lateral maneuvers, simulating real-world scenarios such as emergency lane changes or evasive maneuvers. Several aspects can be analyzed during lane change testing to evaluate the vehicle's handling, stability, and responsiveness.

One crucial focus is on evaluating the vehicle's roll characteristics, which can be represented by parameters like roll angle or roll rate, along with the load transfer developed by the vehicle Roll angle and roll rate measurements provide information about the vehicle's body roll during the lane change. Excessive body roll has the potential to impact both handling stability and driver comfort. Therefore, these parameters serve as valuable indicators of the effectiveness of the vehicle's suspension system.

Figure 34 – Roll and Steer at Lane Change.

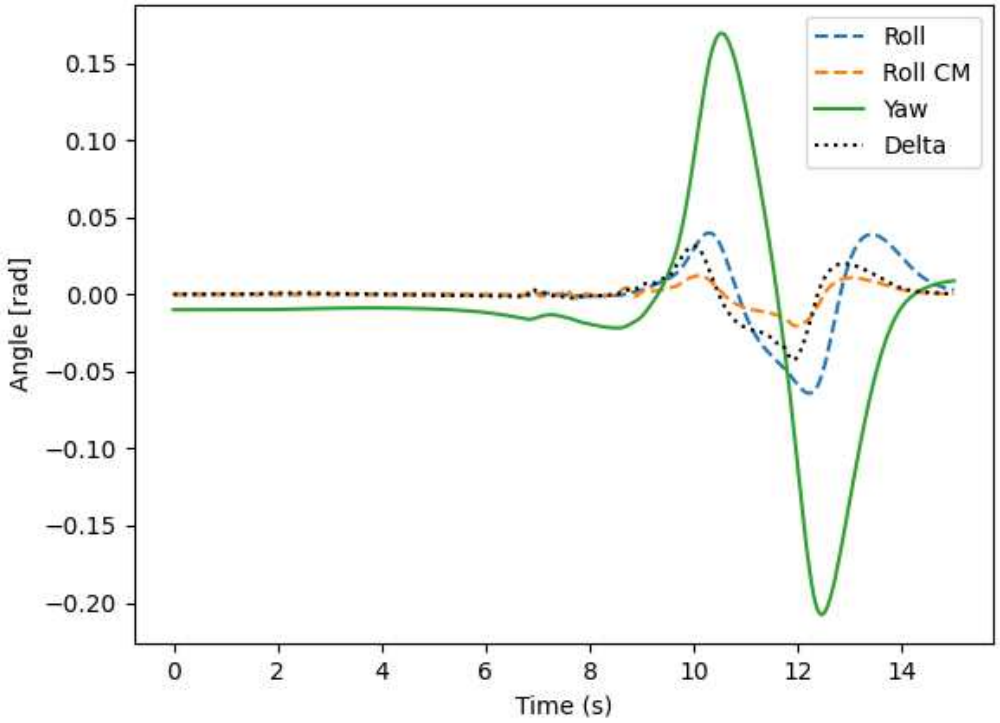

Source: Author

The presentation of roll data from both models during a lane change is showcased in Figure 34. The black dotted line, representing δ delta, indicates the wheel's turning angle in radians and serves as an input variable initiating a change in the vehicle's direction, subsequently altering the Euler angles. The implemented model's data is represented by the blue line, while the roll in the CMmodel is illustrated by the orange dotted line.

Referencing Figure 34, the graph illustrates the roll and yaw angles during a lane change. Both models exhibit similar trends, particularly in roll angles, with a maximum

at the initial peak. The implemented model achieves a maximum of 0.4 radians, whereas CM only incurs a 0.15 radians, nearly three times less.

This consistency is observed at two other peaks, suggesting the possibility of amplifying the roll resistance parameter input for a better alignment with the reference model. Other aspect that can be effect this result is the omission of the anti-roll bar effect in the simulation model constitutes possible source of error. The anti-roll bar plays a key role in diminishing the vehicle's roll angle.

When looking through the wheel forces perspective, first it is seen a strong dependency at x direction with the torque input. Also in the F_y is seen an greater amplification on the external wheels at the front axle. This is a consequences of the weight transference that is capture as forces once the slip calculate and normal forces goes into the magic formula tire model.

Figure 35 – Wheel Forces at Lane Change Manoeuvre.

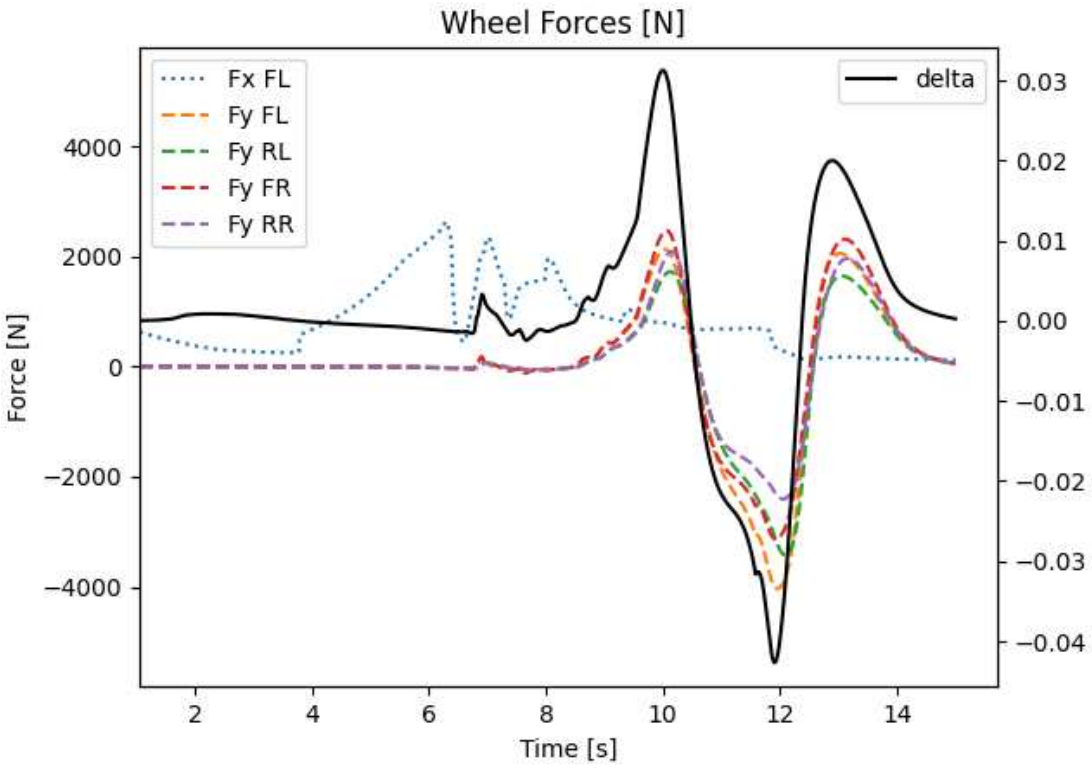

Source: Author

When examining the longitudinal vehicle velocity, comparable results are evident, with the maximum deviation occurring near the peak. The CM model registers $27.75m/s$, while the implemented model records $v_x = 26.20m/s$, representing a 5% error.

In contrast, when analyzing the v_y, which is significantly smaller, the disparity between the models is more pronounced. The implemented model exhibits an almost twofold

Figure 36 – V_x at Lane Change.

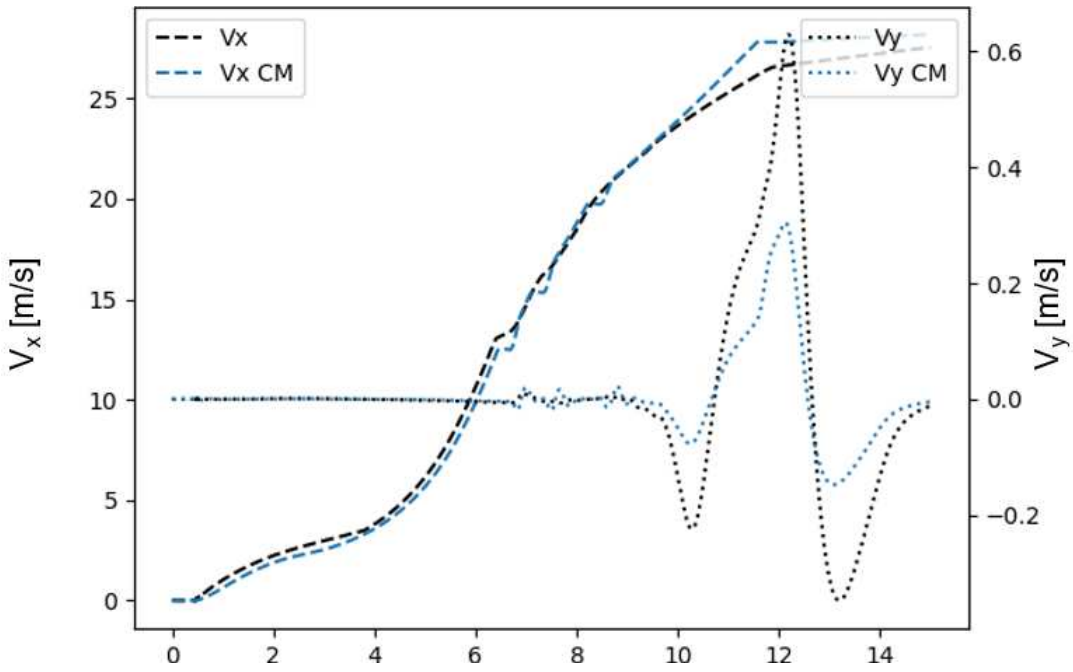

Source: Author

difference compared to the CM model, possibly attributed to yaw and roll deviations between the models, influencing the deviation in v_y. As a result, the implemented model demonstrates a more understeered behavior. This variance could potentially be addressed through the implementation and fine-tuning of an anti-roll bar.

Finally, the change in roll and yaw rate is depicted for the implemented and CM models, respectively showed at Figure 37. It is evident from the illustration that the implemented model offers a smoother prediction of the roll rate, exhibiting minimal fluctuations. In contrast, the CM model displays oscillations at a higher frequency, suggesting potential consideration of compliance effects or similar phenomena in this model. Similar patterns emerge in the analysis of yaw rate, further supporting the hypothesis. Additionally, there is evidence indicating stiffer resistance values for yaw and roll movements, as observed in the CM model.

4.5 OPTIMIZATION RESULTS

To exemplify the potential and applicability of the optimization process in the vehicle dynamic model, it was chosen to optimize parameters with strong influence at the powertrain. This optimization aims to enhance the alignment with longitudinal velocity. Initially, we explored the sensitivity of the model's response to specific parameters anticipated to significantly impact v_x. The parameters under consideration are mentioned at the Table 6 with the initial and the optimized value:

Figure 37 – Roll and Yaw Rate at Lane change.

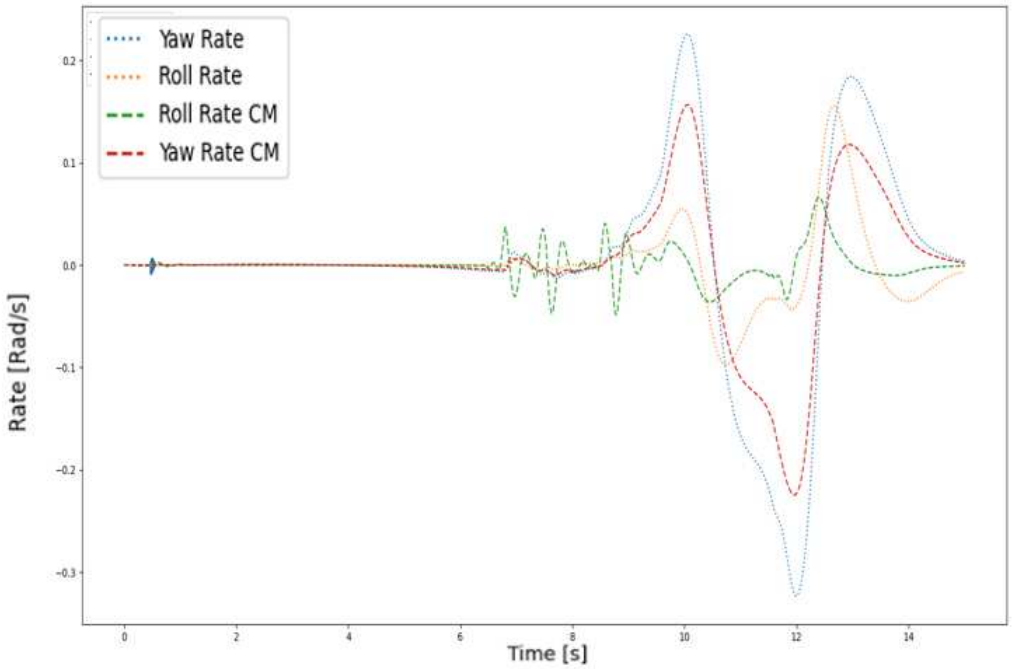

Source: Author

Table 6 – Optimized Powertrain Parameters

Optimized Parameter	**Initial Value**	**Limits**	**Opt. Value**	**Unit**
Gear Box Inertia	1.0	(0 - 2)	1.82440531	Kgm^2
Engine Inertia	5.22	(1 - 5)	2.89029969	Kgm^2
Wheel Inertia	25	(15 - 40)	31.42889341	Kgm^2
Drive Shaft Inertia	0.1	(0 - 1)	0.62667492	Kgm^2

Table 7 – Input Powertrain Parameters

Input name	**Used input**
Maximum Iteration Number	100
population Size	50
Mutation Probability	0.1
Elite Ratio	0.01
Crossover Probability	0.5
Parents Portion	0.3
Crossover Type	Uniform
Max Iteration Without Improv	50

Besides the initial guess other input parameter are essential to apply the GA algorithm. Those are presented at Table 7. The choice of the input value was to start with the standard values with Maximum Iteration Number of 100 and population Size of 50. However, to enhance code speed, both inputs were subsequently halved.

Figure 38 – Longitudinal velocity comparison.

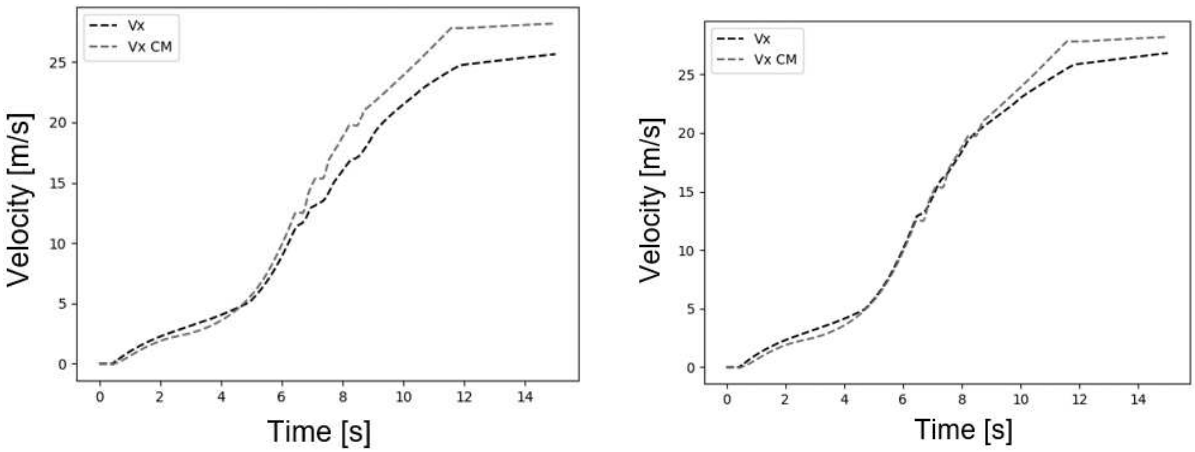

(a) Default (b) Optimized

Source: Author

As result the new value of the select parameter came as an output. The best solution found is illustrated at Table 6 at the optimized value column. The effective result of the optimization process is showed at the vehicle longitudinal speed graphic comparison between initial value result and after optimization at the Figure 38.

An attenuation in the disparity between the CM base model and the applied model was noted. From 0 to 10 m/s, the distinction became nearly imperceptible, whereas the peak deviation, observed around the $25m/s$ threshold, decreased from $3.75m/s$ to $1.25m/s$. Overall, this script conducts an optimization process using a genetic algorithm to find optimal parameters for the vehicle inertia's in power train module based on simulation data.

The optimization process seeks to minimize the disparity between the simulated v_x data and the v_x data obtained from the current parameter configuration. Other parameters can be assessed as input and output, depending on the analysis objectives. While this offers significant flexibility, it also requires a high level of expertise from the user to understand how vehicle parameters interrelate and their sensitivity to changes.

5 CONCLUSION

In conclusion, a comprehensive 10 DoF vehicle model which includes ride, handling, and tire model was developed to study of vehicle dynamics. The 10 DoF vehicle model performed standardized maneuver with the help of CM was validated with multiple standardize test maneuver, focusing on longitudinal, lateral and transitory state characteristics over the acceleration and braking, step steer and lane change respectively.

The parameter identification process was executed in two distinct stages. Initially, all essential model parameters—such as the center of mass location, chassis and wheel inertia values, and suspension parameters were directly measured. Parameters beyond our immediate measurement capabilities, such as those for the combined slip 1989 Pacejka tire model, were identified through extensive literature review. Subsequently, a series of validation tests were conducted to assess the model's accuracy and refine parameters inferred from existing literature.

It was carried out analysis for lateral acceleration, yaw rate, roll angle and tire slip angle responses. From the 10 DoF model validation results, the trend between the simulation and experiment was similar with small difference in the magnitude. In longitudinal, lateral, and combined testing, the simulated model results closely matched reference model. After optimizing powertrain inertial parameter the results achieve longitudinal velocity achieve from 0 to $10m/s$, the distinction became nearly imperceptible, whereas the peak deviation, observed around the $25m/s$ threshold, decreased from $3.75m/s$ to $1.25m/s$ The validation result has proven the 10 DoF vehicle model can be used represent actual vehicle dynamic behavior. The model demonstrated reasonable fidelity in predicting vehicle velocities and rotational motion, offering valuable insights into the impact of parameters such as gear change on pitch rate.

The differences arises due to the model simplification such as ignoring anti-roll bar, body flexibility, movement of roll center and also difficulty for the driver to maintain constant vehicle speed during the test maneuver. For any conclusion regardless of the optimization capacities model and it is parameter estimation capability is necessary to run virtual and real test under a range of scenarios to better understand which parameter can be well estimated with the optimization applied. Once the results for the vehicle test were made is possible to speed up the parameter estimation for further developments in car automated driving vehicles.

Tire model apply meet the initial requirements and further optimization to weather condition and pressure and temperature may be integrated. Different weather scenarios as well as car condition can be emulated using the present work, although further investigation with real testing is mandatory to evaluate the capacity in each scenario. In conclusion, the identified model is a reasonably accurate representation of the double lane, step steer testing and can be useful for a quicker parameter estimation under some test cases.

Although further investigation for different weather scenarios should be explored.

Considering all factors, it's clear that despite the current enthusiasm for automated driving applications and the strides made, there is still a significant road ahead. Overcoming challenges related to infrastructure, cost, and technical maturity is essential. However, reaching the required level of maturity for widespread commercial application of autonomous systems is achievable with the development of techniques and infrastructure that can support these applications economically.

5.1 FUTURE WORK

Future work to enhance the full vehicle dynamic model encompasses several key areas, notably the refinement of tire and suspension models. While the current combined slip tire models offer accuracy, advancements in the Pacejka model, addressing aspects like normal load change rates, camber thrust, temperature fluctuations, and road friction, promise to enhance transient response fidelity. However, comprehensive parameter identification through extensive testing is imperative for optimal utilization.

Regarding the suspension model, the current framework utilizes linear springs and linear dampers. However, there is potential for improvement through the exploration of additional components such as anti-roll bars and kinematic considerations, which could enhance the model's fidelity and accuracy in representing vehicle dynamics.

In pursuit of expedited progress and broader applicability, the following steps are proposed for improving concept implementation:

- Enhancing modularity to enable simultaneous enhancement of multiple modules and interchangeability between different types of powertrains, tire models, and suspension systems.
- Tailoring powertrain models to accurately reflect modern propulsion systems, with specific attention to hybrid and electric vehicles.
- Implementing additional parameter optimizations, such as refining tire parameters, to enhance model fidelity.
- Exploring alternative modeling techniques, including the utilization of neural networks, to expand the modeling capabilities and improve accuracy.
- Streamlining the codebase to enable efficient testing across a variety of scenarios with a friendly interface.
- Expanding tire modeling to incorporate various terrain conditions and account for factors like pressure and temperature, thereby ensuring a more comprehensive representation.

Addressing these aspects will enable the full vehicle dynamic model to evolve towards greater accuracy and effectiveness in simulating real-world driving conditions.

REFERENCES

[1] Hervé Abdi et al. "The method of least squares". In: *Encyclopedia of measurement and statistics* 1 (2007), pp. 530–532.

[2] Abdussalam Ali Ahmed and A.F. Saleh Alshandoli. "Using Of Neural Network Controller And Fuzzy PID Control To Improve Electric Vehicle Stability Based On A14-DOF Model". In: *2020 International Conference on Electrical Engineering (ICEE)*. 2020, pp. 1–6. DOI: 10.1109/ICEE49691.2020.9249784.

[3] Allan Bonnick. *Vehicle Dynamics Compendium*. Tech. rep. Chalmers University of Technology, 2017.

[4] Sindhura Buggaveeti et al. "Longitudinal Vehicle Dynamics Modeling and Parameter Estimation for Plug-in Hybrid Electric Vehicle". In: *SAE International Journal of Vehicle Dynamics, Stability, and NVH* 1.2 (2017), pp. 289–297. ISSN: 23802162. DOI: 10.4271/2017-01-1574.

[5] CARLA. *introduction- CARLA Simulator*. 2023. Available on: https://carla.readthedocs.io/en/latest/start_introduction/ (visited on 11/28/2023).

[6] CarMaker. *car*. 2023. Available on: https://ipg-automotive.com/en/products-solutions/software/carmaker/ (visited on 11/28/2023).

[7] CarSim. *CarSim Information-Overview*. 2023. Available on: https://www.carsim.com/products/carsim/ (visited on 11/28/2023).

[8] Abel Castro, Georg Rill, and Hans I. Weber. "Development of a Robust Integrated Control System to Improve the Stability of Road Vehicles". In: *Multibody Mechatronic Systems*. Ed. by João Carlos Mendes Carvalho et al. Cham: Springer International Publishing, 2018, pp. 506–516.

[9] Di Chen, C. Danielson, and Masahiro Iezawa. "Improving Passenger Comfort by Exploiting Hub Motors in Electric Vehicles: Suspension Modeling". In: (2020). DOI: 10.1115/DSCC2020-3167.

[10] Maikol Funk Drechsler. "Anti-Slip Control With an Actor-Critic Reinforcement Learning Algorithm". PhD thesis. Federal University of Santa catarina, 2019.

[11] Johann Dréo et al. *Metaheuristics for hard optimization: methods and case studies*. Springer Berlin Heidelberg, 2006, pp. 1–367. ISBN: 3-540-23022-X.

[12] Gao Feng, Dongfang Dang, and Yingdong He. "Robust Coordinated Control of Nonlinear Heterogeneous Platoon Interacted by Uncertain Topology". In: *IEEE Transactions on Intelligent Transportation Systems* 23.6 (2022), pp. 4982–4992. DOI: 10.1109/TITS.2020.3045107.

[13] Feng Gao et al. “A Simplified Vehicle Dynamics Model for Motion Planner Designed by Nonlinear Model Predictive Control”. In: *Applied Sciences* 11.21 (2021). ISSN: 2076-3417. DOI: 10.3390/app11219887. Available on: https://www.mdpi.com/2076-3417/11/21/9887.

[14] Matthew Van Gennip. “Vehicle Dynamic Modelling and Parameter Identification for an Autonomous Vehicle”. In: (2018).

[15] G. Genta and L. Morello. *The Automotive Chassis: Volume 2: System Design*. Mechanical Engineering Series. Springer Netherlands, 2008. ISBN: 9781402086731. Available on: https://books.google.com.br/books?id=s4VfNQEACAAJ.

[16] Giancarlo. Genta. *The Automotive Chassis Volume 1: Components Design*. eng. 2nd ed. 2020. Mechanical Engineering Series. Cham: Springer International Publishing, 2020. ISBN: 3-030-35635-3.

[17] O. Gietelink et al. “Development of advanced driver assistance systems with vehicle hardware-in-the-loop simulations”. In: *Vehicle System Dynamics* 44 (2006), pp. 569–590. DOI: 10.1080/00423110600563338.

[18] Thomas D Gillespie. *Fundamentals of vehicle dynamics*. Tech. rep. SAE Technical Paper, 1992.

[19] J. Happian-Smith. *An Introduction to Modern Vehicle Design*. Butterworth-Heinemann, 2001. ISBN: 9780750650441. Available on: https://books.google.com.br/books?id=36kg2DJiy7cC.

[20] Bernd Heißing and Metin Ersoy. “„Chassis handbook: Fundamentals, driving dynamics, components, mechatronics, perspectives (ATZ/MTZ-Fachbuch)””. In: *Vieweg-Teubner Verlag* (2011), pp. 61–63.

[21] Leonhard Hermansdorfer et al. “End-to-end neural network for vehicle dynamics modeling”. In: *Colloquium in Information Science and Technology, CIST* 2020-June (2020), pp. 407–412. ISSN: 23271884. DOI: 10.1109/CiSt49399.2021.9357196.

[22] Márton Tamás Horváth et al. “Vehicle-In-The-Loop (VIL) and Scenario-In-The-Loop (SCIL) Automotive Simulation Concepts from the Perspectives of Traffic Simulation and Traffic Control”. In: *Transport and Telecommunication* 20.2 (2019), pp. 153–161. ISSN: 14076179. DOI: 10.2478/ttj-2019-0014.

[23] Rolf Isermann. “Parameter and State-Estimation Methods for Vehicle Dynamics”. In: Jan. 2022, pp. 235–267. ISBN: 978-3-642-39439-3. DOI: 10.1007/978-3-642-39440-9_10.

[24] *Passenger cars – Test track for a severe lane – Test track for a severe lane – Part 1: Double lane-change*. Standard. Geneva, CH: International Organization for Standardization, 2018.

[25] *Passager cars – Steady-state circular driving behaviour – Open-loop test methods*. Standard. Geneva, CH: International Organization for Standardization, 2021.

[26] *Road vehicles – lateral transient response test methods – Open-loop test*. Standard. Geneva, CH: International Organization for Standardization, 2011.

[27] Jeong hwan Jeon et al. "Optimal motion planning with the half-car dynamical model for autonomous high-speed driving". In: *2013 American Control Conference*. 2013, pp. 188–193. DOI: 10.1109/ACC.2013.6579835.

[28] Werner Schiehlen (auth.) Karl Popp. *Ground Vehicle Dynamics*. 1st ed. Springer-Verlag Berlin Heidelberg, 2010. ISBN: 3540240381.

[29] Phil Kim. "Neural Network". In: *MATLAB Deep Learning: With Machine Learning, Neural Networks and Artificial Intelligence*. Berkeley, CA: Apress, 2017, pp. 19–51. ISBN: 978-1-4842-2845-6. DOI: 10.1007/978-1-4842-2845-6_2. Available on: https://doi.org/10.1007/978-1-4842-2845-6_2.

[30] Hemanth Kolera-Gokula. *Improvements to FE Parts for easier flex body workflows and more productivity*. LinkedIn, Accessed on April 02, 2024. 2021. Available on: https://simulatemore.mscsoftware.com/category/products/adams-products/.

[31] Jason Kong et al. "Kinematic and dynamic vehicle models for autonomous driving control design". In: *IEEE Intelligent Vehicles Symposium, Proceedings* 2015-Augus.June (2015), pp. 1094–1099. DOI: 10.1109/IVS.2015.7225830.

[32] Yokesh Kumar. *Genetic algorithm in casting gating system design*. LinkedIn, Accessed on April 09, 2024. 2023. Available on: https://www.linkedin.com/pulse/genetic-algorithm-casting-gating-system-design-yokesh-kumar-d1vkc/.

[33] Antonino Laudani et al. "On Training Efficiency and Computational Costs of a Feed Forward Neural Network: A Review". In: *Computational Intelligence and Neuroscience* 2015 (2015). DOI: 10.1155/2015/818243.

[34] Rudolf Limpert. *Brake design and safety*. SAE, 2011.

[35] A. Mazilu and I. Preda. "Kinematic Optimization of the Rack and Pinion Steering-System of an Automobile: An Example". In: Publishing House of Transilvania University, 2016. Available on: https://www.researchgate.net/publication/311309543_Kinematic_Optimization_of_the_Rack_and_Pinion_Steering-System_of_an_Automobile_An_Example.

[36] William F. Milliken and Douglas L. Milliken. *Race Car Vehicle Dynamics*. Great Britain: Society of Automotive Engineers Inc., 1996.

[37] D Moldovanu, A Csato, and N Bagameri. "Study regarding the implementation of an Ackerman steering geometry in MATLAB". In: *IOP Conference Series: Materials Science and Engineering* 568.1 (2019), p. 012092. DOI: 10.1088/1757-899X/568/1/012092. Available on: https://dx.doi.org/10.1088/1757-899X/568/1/012092.

[38] Ferhat Ozcan and Sezgin Ersoy. "Analysis of the vehicle: applying finite element method of 3D data". In: *Mathematical Models in Engineering* 7 (Dec. 2021). DOI: 10.21595/mme.2021.22328.

[39] H.B. Pacejka. *Tyre and Vehicle Dynamics*. Automotive engineering. Butterworth-Heinemann, 2006. ISBN: 9780750669184. Available on: https://books.google.com.br/books?id=wHlkbBnu9FEC.

[40] Changwoo Park, Seunghwan Chung, and Hyeongcheol Lee. "Vehicle-in-the-Loop in Global Coordinates for Advanced Driver Assistance System". In: *Applied Sciences* 10 (Apr. 2020), p. 2645. DOI: 10.3390/app10082645.

[41] Philipp Rosenberger et al. "Analysis of Real World Sensor Behavior for Rising Fidelity of Physically Based Lidar Sensor Models". In: *2018 IEEE Intelligent Vehicles Symposium (IV)*. 2018, pp. 611–616. DOI: 10.1109/IVS.2018.8500511.

[42] Andrius Ružinskas and Henrikas Sivilevičius. "Investigation and comparison of tires perfomance on ice". In: *10th International Conference on Environmental Engineering, ICEE 2017* April (2017), pp. 27–28. DOI: 10.3846/enviro.2017.146.

[43] Carsten Schedlinski and Michael Link. "A SURVEY OF CURRENT INERTIA PARAMETER IDENTIFICATION METHODS". In: *Mechanical Systems and Signal Processing* 15.1 (2001), pp. 189–211. ISSN: 0888-3270. DOI: https://doi.org/10.1006/mssp.2000.1345. Available on: https://www.sciencedirect.com/science/article/pii/S0888327000913451.

[44] D. Schramm, M. Hiller, and R. Bardini. *Vehicle Dynamics: Modeling and Simulation*. Springer Berlin Heidelberg, 2014. ISBN: 9783540360452. Available on: https://books.google.com.br/books?id=SXIqBAAAQBAJ.

[45] Joga Setiawan, Mochamad Safarudin, and Amrik Singh. "Modeling, simulation and validation of 14 DOF full vehicle model". In: Dec. 2009, pp. 1–6. DOI: 10.1109/ICICI-BME.2009.5417285.

[46] Carrol Smith. *TUNE TO WIN*. AERO PUBLISHERS, INC, 1978. ISBN: 0-87938-071-3.

[47] Amir Masoud Soltani. "Low Cost Integration of Electric Power-Assisted Steering (EPAS) with Enhanced Stability Program (ESP)". PhD thesis. Cranfield University, 2015.

[48] Zsolt Szalay, Zoltán Hamar, and Peter Simon. "A Multi-layer Autonomous Vehicle and Simulation Validation Ecosystem Axis: ZalaZONE". In: *Intelligent Autonomous Systems 15*. Ed. by Marcus Strand et al. Cham: Springer International Publishing, 2019, pp. 954–963.

[49] M. Tsogas et al. "Detection of maneuvers using evidence theory". In: *2008 IEEE Intelligent Vehicles Symposium* (2008), pp. 126–131. DOI: 10.1109/IVS.2008.4621230.

[50] Yang Ying, Liu Weiguo, and Isah Sagir Tukur. "Performance analysis and simulation of vehicle electronic stability control system". In: *Proceedings - 14th International Symposium on Distributed Computing and Applications for Business, Engineering and Science, DCABES 2015* (2016), pp. 415–418. DOI: 10.1109/DCABES.2015.110.

Appendix

APPENDIX A – GIT HUB REPOSITORY

https://github.com/PauloRafaelAB/VehicleDynamic